



This document is a postprint version of an article published in Marine Environmental Research © Elsevier after peer review. To access the final edited and published work see <https://doi.org/10.1016/j.marenvres.2020.105220>

Document downloaded from:



1

2 ***Pinna nobilis* in suboptimal environments are more**  
3 **tolerant to disease but more vulnerable to severe**  
4 **weather phenomena**

5

6 Patricia Prado<sup>1\*</sup>, Amalia Grau<sup>2, 3</sup>, Gaetano Catanese<sup>2, 3</sup>, Pep Cabanes<sup>1</sup>,  
7 Francesca Carella<sup>4</sup>, Margarita Fernández-Tejedor<sup>1</sup>, Karl B. Andree<sup>1</sup>, Teresa  
8 Añón<sup>5</sup>, Sebastián Hernandis<sup>5</sup>, José Tena<sup>5</sup>, José Rafael García-March<sup>5</sup>

9

10 <sup>\*1</sup>IRTA-Sant Carles de la Ràpita. Ctra. Poble Nou Km 5.5, 43540 Sant Carles de la Ràpita,  
11 Tarragona, Spain

12 <sup>2</sup>Laboratori d'Investigacions Marines i Aqüicultura, (LIMIA) - Govern de les Illes Balears, Av.  
13 Gabriel Roca 69, 07158 Port d'Andratx - Mallorca (Spain).

14 <sup>3</sup>Instituto de Investigaciones Agroambientales y de Economía del Agua, (INAGEA) (INIA-  
15 CAIBUIB). Ctra. Valldemossa km. 7,5 Ed. Edifici Guillem Colom Casanoves, 07122 Palma de  
16 Mallorca - Illes Balears

17 <sup>4</sup>University of Naples Federico II, Department of Biology, Complesso di MSA, 80126 Naples,  
18 Italy

19 <sup>5</sup>Institute of Environment and Marine Science Research (IMEDMAR-UCV). Universidad Católica  
20 de Valencia SVM, Avda. del Puerto s/n, 03710 Calpe, Alicante, Spain

21

22 ABSTRACT

23 We examined a disease outbreak of the fan mussel, *Pinna nobilis* (L.), in the Alfacs Bay  
24 (South Ebro Delta, Spain) during a period of two years in three zones exposed to a summer  
25 salinity gradient resulting from agricultural freshwater discharges and distance to the open  
26 sea. Long-term monitoring was also conducted in Fangar Bay (North Ebro Delta), featuring  
27 lower salinities and no evidence of disease. Results showed that the salinity gradient of Alfacs  
28 Bay (37.4 to 35.7) was associated to cumulative mortality (100% near the mouth, 43% in  
29 middle regions, and 13% in inner regions), thus hindering the spread of pathogens. Young  
30 specimens showed to be more tolerant to disease than large adults but become vulnerable  
31 over time. In Fangar Bay, lower salinities (30.5 to 33.5) prevented the disease but individuals  
32 were highly vulnerable to Storm Gloria which caused 60% mortality in 3 weeks, and ~100% in 6  
33 weeks.

34

35 *Keywords:* Confined waters; salinity; suspended solids; MMEs; Haplosporidium; Mycobacteria;  
36 storm effects; pen shell; Mediterranean

37

38 **1. Introduction**

39 The pen shell *Pinna nobilis* L. is an endemic Mediterranean bivalve distributed across a wide  
40 type of coastal environments including coastal and estuarine ecosystems (Butler et al., 1993;  
41 Kersting et al., 2019). In open coastal waters, the distribution and abundance of the species is  
42 greatly associated to that of seagrass meadows of *Posidonia oceanica*, which has been  
43 indicated as its optimal habitat (Guallart and Templado, 2012). Yet, the species has also been  
44 shown to occur in some coastal lagoons (De Gaulejac, 1995; Katsanevakis, 2006; Zakhama-  
45 Sraieb et al., 2011; Russo, 2017; Belando et al., 2015) and estuarine bays (Addis et al., 2009;  
46 Prado et al., 2014, 2020), often dominated by other soft-bottom habitats such as *Cymodocea*  
47 *nodosa* and *Zostera* spp. seagrass meadows, macroalgal beds of *Caulerpa prolifera* and/or  
48 sandy and muddy shores. Populations in both types of environments are exposed to  
49 contrasting environmental conditions that may shape their abundance, distribution, age  
50 structure and overall vulnerability and recovery from severe weather phenomena. In the open  
51 sea, the species distribution and size structure are strongly influenced by wave action and  
52 density of seagrass (*P. oceanica*) meadows that determine the intensity of drag forces (García-  
53 March et al., 2007a, b; Hendriks et al., 2011). The species can be found from ca. 5 to 60 m  
54 (Butler et al. 1993; García-March et al., 2007b), although higher abundances are usually  
55 reported from 10 m to up to 38 m (García-March et al., 2007b; Rouanet et al., 2015). In  
56 contrast, confined waters provide a more sheltered environment, and populations have been  
57 found to peak at less than 1 m (Zakhama-Sraieb et al. 2011; Russo, 2017; Prado et al., 2014), 2-  
58 5 m (Coppa et al., 2013) and up to 11-13 m depth (Katsanevakis 2006, 2007), possibly  
59 depending on the influence of local geomorphology in recruitment patterns (see Prado et al.,  
60 2020a).

61 *Pinna nobilis* has been indicated to withstand a wide range of water temperatures from ca.  
62 7 to 28 °C but to have a narrow window of optimal salinities ranging from 34 to 40 (Butler et  
63 al., 1993). Open sea populations in the Mediterranean dwell in a relatively stable environment

64 with small salinity fluctuations of around 36-39, that overlap the optimal range of the species.  
65 In contrast, pen shell populations in some coastal lagoons and estuarine bays, may have to  
66 persist in salinity conditions that are *a priori* suboptimal for the development of the species.  
67 For instance, in the hypersaline lagoon of the Mar Menor (SW Spain) pen shells endure salinity  
68 ranges between 42 and 47 (Fernández-Torquemada and Sánchez-Lizaso, 2011), and similar  
69 ranges from 36 to 51 are attained in the Ghar El Melh lagoon (N-E Tunisia) (Zakhama-Sraieb et  
70 al., 2011). In the lower salinity range, pen shells in Fangar Bay (Ebro Delta) are exposed to  
71 annual values ranging from 20 to 35 associated to important seasonal discharges of freshwater  
72 from rice agriculture (Carrasco et al., 2008). Despite these suboptimal conditions, massive,  
73 occasional recruitment events during favorable periods may lead to the establishment of  
74 thousands of individuals such as populations reported for the Mar Menor, Venice Lagoon, or  
75 Alfacs Bay (Prado et al., 2014; Russo, 2017; Giménez-Casalduero et al., 2020). Yet, these  
76 populations may also be more vulnerable to changes in the confined water bodies resulting  
77 from persistent urban and agricultural pressures (e.g. García-Pintado et al., 2007) and/ or great  
78 storms and heavy rains, typically reducing salinity and providing large quantities of silts and  
79 sediments (Isla, 2009). For instance, mortalities of cultivated bivalves such as mussels and  
80 cockles have been reported as a result of burial by storm-eroded biodeposits (Landahl, 1988;  
81 Nehls and Thiel, 1993; Dare, 2004), but the impact in other non-commercial species may have  
82 passed unnoticed.

83 Recently, *Pinna nobilis* has been listed as a “critically endangered” species by the Spanish  
84 government (BOE 251-14181, 2018), and the International Union for Nature Conservation  
85 (IUCN; Kersting et al., 2019). Mortalities close to 100% of the populations have been reported  
86 along the entire Mediterranean Spanish coast and other Mediterranean countries such as  
87 France, Italy, Greece, Tunisia, Croatia, Cyprus, and Turkey (Cabanellas-Reboredo et al., 2019),  
88 which are presumably due to the cooperation of a parasitic disease by *Haplosporidium pinnae*  
89 (Catanese et al., 2018) and bacterial pathogens such as *Mycobacterium* sp. (Carella et al.,

90 2019). At present, only one population along the Spanish Mediterranean coast located in  
91 Fangar Bay (North Ebro Delta, containing hundreds of individuals) remains clean of pathogens.  
92 Just a few kilometers south, the population in Alfacs Bay (South Ebro Delta) was infected in its  
93 more external part in 2018 (García-March et al., 2020a) located next to the open sea and  
94 subjected to higher salinities (Cerralbo et al., 2019). In the other remaining Spanish population  
95 in the Mar Menor, some individuals were positive for the presence of *H. pinnae* after a long-  
96 term (in the order of months) salinity reduction to ca. 39 following a meteorological  
97 phenomenon known as “cold drop” or DANA, the Spanish acronym for isolated depression in  
98 high layers of the atmosphere, causing heavy rains in September of 2019 (Nebot-Colomer et  
99 al., submitted). These infection patterns seem to confirm the disease dispersion model at  
100 salinities of ca. 36.5-39.7 proposed by Cabanellas-Reboredo et al., (2019), and suggests the  
101 importance of preserving extreme abiotic conditions for protecting the last remaining  
102 populations of pen shells.

103 In this work, we evaluate the magnitude and the causes of two mass mortality events  
104 (MME) in the two Ebro Delta populations of *Pinna nobilis* in order to assess the resilience of  
105 the populations and the capacity of open estuarine environments to act as refugia for the  
106 species. The first MME took place in the summer of 2018 in the external part of Alfacs Bay  
107 (South Ebro Delta), while the second one occurred in Fangar Bay (South Ebro Delta) after the  
108 pass of Storm Gloria along the Spanish Mediterranean coast. Environmental data was collected  
109 at different monitoring times, and in the particular case of Fangar Bay, physicochemical  
110 conditions were also followed from two days after Storm until the normalization of conditions  
111 ca. 2 weeks later. In both bays, samples of recently dead individuals and survivors were  
112 collected in order to investigate a possible infection by *Haplosporidium pinnae* and  
113 *Mycobacterium* sp. related to possible lesions at the tissue level. In addition, the overall age  
114 structure of the populations from growth records in empty shells (already available for Alfacs

115 Bay in Prado et al., 2020a) and the size structure of surviving individuals was assessed in order  
116 to evaluate the long-term persistence of the populations.

117

## 118 **2. Materials and Methods**

### 119 *2.1. Study areas*

120 Alfacs and Fangar Bays are semi-enclosed water bodies with freshwater inputs greater than  
121 evaporation, so that their mean salinity is always lower than that of the sea (Delgado, 1987).

122 Both bays have a great economic importance due to the presence of extensive shellfish  
123 aquaculture, particularly of oysters and mussels.

124 Alfacs Bay spreads over ca. 49 km<sup>2</sup> of the south of the Ebro Delta. The northern shore is  
125 bordered by rice fields and receives agricultural discharges (ca. 275 x 10<sup>6</sup> m<sup>3</sup> year<sup>-1</sup>) high in  
126 nutrients and organic matter that cause eutrophication (Llebot et al., 2011; Prado, 2018). The  
127 bay is characterized by a salinity-dominated stratification, with a superficial layer (0 to 2-3 m  
128 deep) of low salinity (30-35) and an outward movement, and a deep salty layer (salinity: 36-38)  
129 with an inward movement (Quijano-Scheggia et al., 2008). The bulk of the *P. nobilis* population  
130 is located in the southern shore of the bay –the Banyà Sandspit–, which stretches along a  
131 shallow platform of 18 km<sup>2</sup> (ca. 700 m wide) at depths from ca. 30 to 130 cm covered by  
132 *Cymodocea nodosa* seagrass meadows (Prado et al., 2014, 2020  
133 ). Densities of *P. nobilis* along the sandspit also follow the superficial summer salinity  
134 gradient (Cerralbo et al., 2019) with higher densities in the outer part of the bay closer to the  
135 bay mouth, and lower in the inner part (Prado et al., 2014).

136 Fangar Bay is comparatively much smaller, covering an area of ca. 12 km<sup>2</sup> of the north of  
137 the Ebro Delta, but receives a similar amount of freshwater than Alfacs Bay (ca. 250 x 10<sup>6</sup> m<sup>3</sup>  
138 year<sup>-1</sup>; Delgado, 1987; Llebot et al., 2011), resulting in vertical stratification but with lower  
139 superficial salinities of ca. 20-35 (Carrasco et al., 2008). Hence, the pen shell population is also  
140 located in the shallow platform (ca. 30 to 60 cm depth) of the sandspit peninsula, but its

141 distribution is mostly restricted to the outer part, closer to the mouth of the bay. The  
142 submerged platform is composed of silty sediments and dominated by the seagrass *C. nodosa*  
143 along with patches of *Zostera noltii*.

144

## 145 *2.2. Assessment of mortality and survival patterns*

146 Long-term and large-scale patterns of pen shell mortality in Alfacs and Fangar bays were  
147 investigated at increasing distances from the opening of the bay between January 2018 and  
148 February 2020. In the much larger Alfacs Bay, three sites were selected, that were  
149 representative of outer (Site 1), middle (Site 2) and inner areas (Site 3) of the bay. At each site,  
150 three monitoring circles of 8 m of diameter were deployed at ca. 50 m apart in order to  
151 capture variability at the smaller spatial scale (Fig. 1a). In Fangar Bay, given the much smaller  
152 size of the population, only three single monitoring circles were deployed in the area with  
153 highest densities of individuals (Fig. 1b). Monitoring circles in Alfacs Bay contained from 14 to  
154 26 animals and 9 to 22 in Fangar Bay. All individuals were marked with PVC tags for easy  
155 identification during following surveys. All circles were in shallow areas (ca. 30 to 90 cm depth)  
156 and were monitored by walking with an aquascope and by snorkeling when necessary to verify  
157 the tag number.

158 In January 2020, two and a half years after a first mortality event occurred in the outer part  
159 of Alfacs Bay (Site 1), an area of 1 ha was randomly selected within the impacted area and an  
160 intensive search of surviving individuals conducted within 40 contiguous transects of 50 x 5 m.  
161 In each transect living and dead young specimens (i.e., 3-year-old individuals from the last  
162 recruitment event in 2017; see Prado et al., 2020a) and large adults were counted. The same  
163 survey was conducted again in late July 2020.

164 An intensive monitoring was conducted to assess mortality patterns in Fangar Bay, which  
165 was severely hit by Storm Gloria on 19<sup>th</sup> to 22<sup>nd</sup> of January 2020. A first survey was conducted  
166 on the 11<sup>th</sup> of February 2020 (20 days after Storm ), and then again on the 4<sup>th</sup> of March (42



167 days after Storm) in order to assess both short-term and medium-term mortality resulting  
168 from direct alterations in physicochemical variables, and the capacity of animals to recover  
169 normal physiological functions. Despite the restricted pen shell distribution of only ca. 2.28 ha  
170 found during in situ evaluation, during the first survey we noticed the occurrence of 4 sub-  
171 areas with contrasting abundances of individuals (young specimens and adults) and survival  
172 rates. In each sub-area, we conducted 15 to 21 transects of 50 x 5 m (up to a total of 77  
173 transects) across the total area of distribution (Fig. 1b). On the first survey date, for each  
174 transect we counted the number of surviving young specimens and adults, the number of  
175 recently dead (still containing some flesh remains and having no epiphytes in the internal  
176 shells) young specimens and adults, and the number of old shells from previous mortalities. On  
177 the second survey over the same exact areas, only the number of surviving young specimens  
178 and adults were counted.

179 In both bays, transects were conducted simultaneously by two persons walking together  
180 and searching within half of the width area.

181

### 182 *2.3. Size-age evaluation of individuals*

183 The size-age structure of pen shells from Alfacs Bay has been previously determined (Prado  
184 et al., 2020a). For Fangar Bay, twenty shells ranging between 31.8 and 43.6 cm long, —  
185 including the entire size variability available in this shallow environment—, were used to  
186 determine the age range of the population and to assess the availability of different cohorts  
187 indicative of recruitment years. All individuals were collected on February 11<sup>th</sup> 2020, twenty  
188 days after Storm Gloria (19<sup>th</sup> to 22<sup>nd</sup> of January 2020) and still contained some tissues in the  
189 process of decomposition, as evidence of recent dead, possibly 1 week earlier. A sample size of  
190 N= 20 has been shown as sufficient for accurate age estimation in population studies (García-  
191 March and Márquez-Aliaga, 2007; García-March et al., 2011; Prado et al., 2020a). Briefly, one  
192 valve was processed to study the record of the posterior adductor muscle scar (PAMS) from

193 the interior of the shell according to García-March et al. (2011). The valve was radially cut  
194 through the PAMS and ca. 8 cm dorso-ventral sections of one side were mounted on slides. A  
195 thick section (ca. 200 µm) of the portion glued to the slide was cut using a low-speed Buehler  
196 Isomet saw. The free surface of the slide preparation was polished to improve observation of  
197 the growth record. From each polished section, the growth record was counted. Missing  
198 records were calculated using the width of the calcite layer in the three oldest records of all  
199 specimens (García-March et al., 2011).

200

#### 201 2.4. Analyses for detection of potential pathogens and lesions

202 Analyses were aimed at the detection of *Haplosporidium pinnae*, which has been reported  
203 as the main cause of mass mortality events of *P. nobilis* across the Mediterranean (Catanese et  
204 al., 2018; Carella et al., 2020) and *Mycobacterium* sp. which has also been associated to  
205 massive pen shell mortality (Carella et al., 2019; 2020).

206 In Alfacs Bay within Zone 1, one recently dead individual and three showing disease  
207 symptoms (N= 4) (i.e., retracted mantle and difficulty to close the valves) were taken to the  
208 laboratory in July 2018 for assessing the presence of pathogens. For Zones 2 and 3, only two  
209 recently dead individuals could be found in August 2018, which were also taken to the  
210 laboratory for analytical purposes. Later in January 2020, three apparently healthy individuals  
211 from Zone 2 and another five from Zone 3 were sacrificed for the evaluation of structural  
212 anomalies of the shell and microbiome analysis, and were also used to assess the presence of  
213 *H. pinnae* and *Mycobacterium* sp. in both areas. An additional sample from Zone 2 was  
214 collected in May 2020 from a recently dead individual found in the area (i.e., final N= 4 in Zone  
215 2 and N= 5 in Zone 3).

216 For Fangar Bay, two recently dead pen shells and three living individuals without disease  
217 symptoms (N= 5) were collected after Storm Gloria. Samples of all individuals were all tested at  
218 the LIMIA using the specific primers HPNF3/HPNR3 for *H. pinnae* (Catanese et al. 2018) and

219 PCR conditions described by López-Sanmartín et al. (2019). For analyses of presence of  
220 *Mycobacterium* sp. we used specific primers (mycgen-f/ mycgen-r) described by Böttlinghaus  
221 et al., (1990) and PCR conditions indicated by Carella et al., (2019).

222 For all individuals from Alfacs Bay (except that found dead in Zone 2 in May 2020), and the  
223 three sacrificed individuals from Fangar Bay, different transverse sections of each tissue,  
224 including gonad, digestive gland, kidney, mantle, and gills were fixed in Davidson's solution and  
225 preserved for a week at room temperature. Subsequently, tissues were dehydrated in  
226 ascendant alcohol series and embedded in paraffin blocks, and 3-4 µm thick sections were cut  
227 with a Microm HM330 rotary microtome and stained with Mayer's hematoxylin and eosin  
228 (H&E) for routine light microscopic examination. Ziehl-Neelsen (ZN) staining was also  
229 performed to detect acid-fast bacteria. Slides were examined under a light microscope  
230 (Olympus DP20 video camera on an Olympus BX51 microscope) for possible presence of  
231 pathogens and detection of structural tissue damage.

232

### 233 *2.5. Measurement of physicochemical variables*

234 Physicochemical (FQ) variables including temperature, salinity, dissolved oxygen, and pH  
235 were measured monthly at each monitoring circle (N= 3 per zone in Alfacs Bay, and N= 3 in  
236 Fangar Bay) during the entire monitoring period from January 2018 to March 2020 using a YSI  
237 6660 multiparametric probe equipped with a 650 MDS data logger.

238 Furthermore, for Fangar Bay, water transparency was estimated from a Secchi disk, and  
239 salinity, temperature, chlorophyll concentrations (spectrophotometer quantification after  
240 acetone extraction) were measured at 0 to 0.5 m depth (at approx. 12 to 13 h) 6 days before  
241 and 2, 5, 12, 19, 26, 33, 40, and 47 days after Storm Gloria hit the Ebro Delta (19<sup>th</sup> to 22<sup>nd</sup> of  
242 January 2020) in the three points within the bay that are regularly surveyed as a part of a  
243 monitoring program of the Catalanian Government for shellfish safety (see  
244 <http://www.marinemonitoring.org>). Since the mortality of the entire population was

245 investigated twice after the storm (20 days, and an additional sample 42 days after), the  
246 temporal evolution of FQ variables together with the presence/absence of pathogens in the  
247 tissues collected, was used to assess the more likely causes of the mortality event. Images of  
248 the entire Catalanian coast before, during and after Storm Gloria are available from the  
249 Cartographic and Geologic Institute (ICGC) of the Catalonia Government  
250 (<https://visors.icgc.cat/costa/#9/41.5374/1.8718>).

251

## 252 *2.6. Analyses of data*

253 Monthly trends in mortality were investigated with RM-ANOVA (repeated measures). For  
254 Alfacs Bay, differences among sites were investigated, whereas for Fangar Bay with a much  
255 smaller area of distribution, circles were used as replicates with no site (between subjects')  
256 effects. Data were log (x+1) transformed and tested for RM-ANOVA assumptions of normality  
257 and sphericity. Yet, since the Mauchly's Test of Sphericity indicated that the assumption of  
258 sphericity had been violated, a Greenhouse-Geisser correction was used.

259 Differences in the abundance of dead and living young specimens (DY and LY) and adults  
260 (DA, LA) within the surveyed area of 1 ha in Alfacs Bay affected by MME at each of the 2  
261 sampling times were investigated with a two-way RM-ANOVA (Condition and Age, fixed factors  
262 with two levels).

263 Mortality patterns in Fangar Bay at the two sampling times after Storm Gloria were  
264 investigated using a one-way RM-MANOVA testing for differences in the abundance of  
265 recently dead and living young specimens (RDY and LY) and adults (RDA and LA) and the  
266 presence of older shells (OS) from dead animals, across the four observed sub-areas.

267 Monthly patterns in the physicochemical variables of Alfacs Bay during the two study years  
268 were assessed with a two-way factorial ANOVA (Time and Zone fixed factors), and those of  
269 Fangar Bay with a one-way ANOVA (Time fixed factor). Significant differences among factor  
270 groups were investigated using Student-Newman-Keuls (SNK) post hoc tests. ANOVA

271 assumptions of normality (chi-squared test) and heteroscedasticity (Cochran's test) of data  
272 were not always achieved by transformation, but the ANOVA F-statistic is still able to provide  
273 robust results (Underwood, 1997). In those instances, however, the risk of making a Type I  
274 error was minimized by setting the level of significance to 0.01. For the remaining analyses, the  
275 critical level of significance was fixed at  $P < 0.05$ . SNK post hoc comparisons were used to  
276 identify significant differences.

277 The association between cumulative mortality patterns across the different zones of Alfacs  
278 Bay during the hottest summer months (July-August 2018 and 2019) and salinity was  
279 investigated with correlation analyses. Repeated measures analyses were conducted with the  
280 SPSS software v. 20, and ANOVAs of FQ variables and correlation analyses were performed  
281 with STATISTICA v. 12.

282

### 283 **3. Results**

#### 284 *3.1. Assessment of mortality and survival patterns*

285 In Alfacs Bay, RM-ANOVA showed significant time differences across the study period  
286 (January 2018 to March 2019), as well as a significant effect of zone and its interaction (Fig. 2a,  
287 Table 1a). A mortality of up to 63% of the individuals occurred in Zone 1 in July 2018, and 98%  
288 were dead one month later (Fig. 2a). Conversely, the lower mortality in Zones 2 and 3 during  
289 the summer of 2018 was mostly attributed to impacts with boat propellers in shallow areas  
290 around the main sand bar of the bay (8 out of 9 individuals found dead) (Fig. 2a). No mortality  
291 was observed in any monitoring circle until the next summer period in 2019, when the last  
292 individual remaining in Zone 1 was found dead, and some mortality was also detected in Zone  
293 2 (ca. 21% in July and 13.7% in August). No more mortality was recorded during the fall and  
294 winter period of 2019-2020, even after the pass of Storm Gloria in late January 2020.

295 The evaluation of the 1 ha area affected by mass mortality in the surroundings of Zone 1 in  
296 January 2020 showed significant differences in the condition of individuals (dead vs. alive), as

297 well as a significant time x condition and time x age x condition interactions (Table 1b, Fig. 2b).  
298 In January, young specimens (recruitment of 2017) showed higher survival than adults (35.6%  
299 vs. 0% of all individuals counted), with a total of 36 individuals found alive within the study  
300 area, but only 8 (7.91%) were still alive by late July 2020 (Fig. 2b).

301 In Fangar Bay, dead individuals showed no apparent effect of hydrodynamic dislodgement  
302 and were all well anchored to the seagrass substrate. RM-ANOVA also indicated significant  
303 time differences, although effects were due to a massive mortality of all individuals in the  
304 three monitoring circles after Storm Gloria (Fig. 3a, Table 2a), with only minor losses registered  
305 in the area during previous monitoring months (3 individuals in two years). Only one individual  
306 was recorded as dead by collision, likely due to this bay having less touristic boat traffic.

307 Monitoring circles were all located in Zone 3, which together with Zone 2 (Fig. 1a), had the  
308 largest number of individuals in the area and recorded the largest number of deaths. Results  
309 from one-way RM-MANOVA showed significant differences in the numbers of living and dead  
310 young specimens and adult individuals among zones, as well as significant differences in time  
311 and zone interactions across pen shell age and condition (Fig. 3b, Table 2b). At the first  
312 sampling time (20 days after Storm), recently dead adults (RDA) were more abundant in Zone 3  
313 (180 individuals), followed by Zone 2 (101 individuals), and then by Zones 4 and 1 (33 and 3,  
314 respectively), which also hosted much lower densities of individuals. Living adults (LA) were  
315 mostly present in Zone 2 (a total of 210 individuals), whereas in the rest of the zones only 1 to  
316 4 were recorded. For young specimens, the bulk of the population was concentrated in Zone 1  
317 (a total of 47 individuals vs. 13 in all the other zones). Finally, the presence of old shells (OS),  
318 was also much higher in Zones 2 and 3 than in Zones 1 and 4, demonstrating that, in the long-  
319 term, those areas have hosted the highest densities of individuals. At the second sampling  
320 time (42 days after Storm), only 12 LA were detected in Zone 2. Overall, the mortality of young  
321 specimens and adults was ca. 60% at the first sampling time and rose to nearly 100% at the  
322 second sampling time.

323

### 324 3.2. Size-age evaluation of individuals

325 The analysis of the growth record (posterior adductor muscle scars) of the empty shells  
326 showed that from the 20 shells cut, 75% were 4-5 years of age, followed by 15% of 6 years,  
327 and 10% of 7 year, this being the maximal age (Fig. 4). A total of 60 young specimens were also  
328 present in the study area and were estimated to be 2-3 years old (shells that were not cut  
329 because growth parameter estimation is not possible with such young shells). The growth  
330 equation for the Fangar Bay [ $L_t = 41.96 \cdot (1 - e^{(-0.39 \cdot (t+0.276)})$ ] shows high K (0.39) and low  
331  $L_\infty$  (41.96 cm), concurring with multiple shell fractures and reconstructions that account for  
332 small maximum sizes. The total number of individuals in the age range of this equation before  
333 Storm Gloria was 533 (RDA and LA).

334

### 335 3.3. Detection of potential pathogens and lesions

336 PCR analyses for the four investigated individuals (one recently dead and 3 with disease  
337 symptoms) collected in Zone 1 (i.e., the region of Alfacs Bay closer to the mouth of the bay) in  
338 July 2018, showed positive results for both *H. pinnae*, and *Mycobacterium* sp. (two individuals  
339 were only positive to *H. pinnae* by PCR, and the four of them were positive to *Mycobacterium*  
340 sp. through both PCR and microscopy). The two recently dead individuals found in Zone 2 and  
341 Zone 3 in August 2018 were also positive for *H. pinnae*. Further, in the case of the individual  
342 from Zone 2, the parasite could only be detected by histology, not by PCR. Among those  
343 individuals collected in January 2020 (N= 3 from Zone 2 and N= 5 from Zone 3), two from Zone  
344 2 resulted positive for *H. pinnae* (one of them only by histology), but not for *Mycobacterium*  
345 sp. The dead individual from May 2020 in Zone 2 was also positive for *H. pinnae* by PCR. None  
346 of the individuals from Zone 2 or 3 were positive for the presence of *Mycobacterium* sp. either  
347 by PCR or histology.

348 In Fangar Bay, the five individuals investigated (2 recently dead examined by PCR and 3  
349 sacrificed examined by both PCR and histology) after Storm Gloria were all negative for both *H.*  
350 *pinnae*, and *Mycobacterium* sp. The three individuals sacrificed after Storm Gloria showed a  
351 normal digestive gland with no evidence of *H. pinnae*, *Mycobacterium* sp., or other bacterial  
352 infections (Fig. 5a,b). However, individuals displayed a regressing female phase of gonad  
353 maturation, similar to that observed in the post-spawning phase of a normal annual  
354 reproductive cycle, with remaining oocytes after their release in late summer (Prado et al.,  
355 2020a; Deudero et al., 2017) but, without this actually occurring (Fig. 5c,d). When regression  
356 occurred, the first individual was in a previtellogenic stage, whereas the second and third  
357 individuals were already in a more advanced vitellogenic stage. Only few oocytes were  
358 observed remaining attached to the developing gonadal follicle, and the majority of them were  
359 detached and phagocyted by hemocytes (Fig. 5c,d), suggesting a limited reproductive capacity  
360 during the current year, at least at the beginning of the reproductive season.

361

#### 362 3.4. Physicochemical variables

363 In Alfacs Bay, all investigated variables showed important variations across monthly study  
364 dates, as well as significant Date per Zone interactions (Table 3). For temperature, maximums  
365 of ca. 27-30 °C occurred in July-August, and minimum of ca. 9.5 to 14 °C in January-February,  
366 with non-significant differences between study zones (Fig. 6a, Table 3a). Salinity also showed  
367 important temporal differences which are attributed to seasonal rainfall and to freshwater  
368 discharges from rice cultivation, with annual maximums of ca. 37 and minimums of ca. 33,  
369 excepting a lower value of  $32.16 \pm 0.03$  recorded in January 2020, after Storm Gloria (Fig. 6b,  
370 Table 3b). However, in the case of salinity there was also a significant zone effect, with slightly  
371 higher values (by ca. 0.6 over the entire study period) in Z1 closer to the mouth of the bay, and  
372 expectedly lower values in Z2 and Z3. Most importantly, the magnitude of those differences  
373 was higher during the summer months (June-August 2018 and 2019; see Fig. 6b), when



374 *Haplosporidium pinnae* is more infective due to high temperature. Dissolved oxygen was high  
375 in the area, with values ranging from ca. 77 to 123% of saturation, but despite significant  
376 temporal and temporal x zone variability, no clear seasonal or zone pattern could be observed  
377 (Fig. 6c, Table 3c). The pH ranges varied between minimums of ca.7.3 to 7.6 in September  
378 2018 and April 2019, and maximums of ca. 8.3 to 8.5 in June 2018 and October 2019 (Fig. 6d,  
379 Table 3d). Significantly higher pH values were detected in Z3 in July 2019, whereas lower  
380 values were observed in Z1 in August-September 2019 (Fig. 6d).

381 A positive association was detected between cumulative patterns of pen shell mortality  
382 across the three study zones and the salinity ( $R^2= 0.652$ ,  $df= 35$ ,  $F= 63.795$ ,  $p= 2.62 \cdot 10E^{-9}$ )  
383 recorded during the months of July and August (Fig. 7).

384 In Fangar Bay, significant temporal variability was observed for temperature, salinity, and  
385 dissolved oxygen, but not for pH (Table 3e-h). For temperature, the temporal profile was very  
386 similar to that of Alfacs Bay, although with slightly higher maximums and lower minimums (27  
387 to 30 °C and 7 to 13 °C, respectively; Fig. 6e, Table 3e). The salinity was lower than in Alfacs  
388 Bay, with values ranging from ca. 27 to 36, although a minimum of  $11.05 \pm 0.36$  was observed  
389 after Storm Gloria (Fig. 6f, Table 3f). Dissolved oxygen showed a clearer seasonal variability  
390 compared to Alfacs Bay, with minimums of ca. 88-89% during the summer period and  
391 maximums of ca.100-113% in winter (Fig. 6g, Table 3g).

392 At the shorter temporal scale (before and after Storm Gloria), the only FQ variables, which  
393 experienced a sharp change were salinity and the water transparency given by the Secchi disc  
394 measurements (Fig. 8A-F). Salinity was reduced from ca. 28 to 11 just after Storm Gloria with  
395 normal values being again recorded 12 days later, although a new minimum was recorded  
396 again in March (Fig. 8B). Similarly, the visibility of the Secchi disc was greatly reduced from 3.4  
397 to 0.34 m after Storm and normal values were also recorded 12 days later (Fig. 8E). This result  
398 of strong reduction of water transparency confirms satellite images from the ICGC institution  
399 showing elevated water turbidity after Storm Gloria.

400

401 **4. Discussion**

402 The pen shell populations of the Ebro Delta are, together with that from Mar Menor Lagoon  
403 (this study; Giménez-Casalduero et al., 2020), the only ones in Spanish waters that have  
404 persisted, –totally or partially–, after MMEs caused by the rapid spread of *Haplosporidium*  
405 *pinnae* (Vazquez-Luis et al., 2018; Cabanellas-Reboredo et al., 2019). Yet, similar patterns of  
406 survival are being observed in confined waters across other Mediterranean regions such as  
407 lagoons along the French Occitan Coast and Corse (Simide et al., 2019; García-March et al.,  
408 2020a; Foulquié et al. 2020), the Venice lagoon in Italy (Carella, pers. observ.), and the  
409 Thermaikos Gulf in Greece (Lattos et al., 2020). In Alfacs Bay, the summer salinity gradient  
410 (from 37.4 to 35.7) showed to be significantly associated to observed patterns of cumulative  
411 mortality. Although this salinity range is too narrow to prevent the infection of the population,  
412 it seems to be effectively hindering the spread of the parasite compared to open water  
413 conditions, as predicted by the dispersion model at salinities above 36.5 (Cabanellas-Reboredo  
414 et al., 2019). However, it is important to remark that salinities during the rest of the year also  
415 range from 34 to 36 in external parts of Alfacs Bay, and from 32 to 36 in intermediate and  
416 internal parts of the bay (see also Cerralbo et al., 2019), which might contribute to further  
417 obstruct the spread of the parasite and the rate of disease transmission. In fact, although in  
418 open waters *H. pinnae* has been reported to cause disease at temperatures as low as 13.5 °C  
419 (García-March et al., 2020a), major mortalities in Alfacs Bay were constricted to periods above  
420 27 °C mostly during July and August. Other extant estuarine fan mussel populations (usually  
421 between ca. 30 to 40) such as those in the Diane and Thau Lagoons in France (Simide et al.,  
422 2019; Foulquié et al. 2020) might be exposed to a similar seasonal risk as those in Alfacs Bay,  
423 although the more restricted connection with the open sea might provide an additional  
424 protection. Given this more constricted period for high risk of disease and its apparently lower  
425 transmission in waters below salinity of 36.5, the persistence of estuarine populations

426 confronted with potential infections will be largely dependent on the ratio between mortality  
427 and new recruitment. In Alfacs Bay, Prado et al. (2020) showed that the age structure of the  
428 population is dominated by individuals of the  $8 \pm 1$  year-old class with a maximum age of 15  
429 years and only one major recruitment event in 11 years followed by periods of slow population  
430 growth. Also unsettling is the fact that the natural pattern of distribution and abundance of  
431 individuals across the bay is inversely related to the salinity gradient (Cerralbo et al., 2019;  
432 Prado et al., 2014), suggesting that larval viability may, to some extent, be hindered by  
433 agricultural discharges in areas that are safer from the parasite (Prado et al., 2020a). Yet, there  
434 is also genetic evidence that the population in Alfacs Bay is source of larvae for more distant  
435 populations in the Balearic Islands (Wesselmann et al., 2018), advocating that the population is  
436 capable of successful larval export.

437       Among other factors conditioning the persistence of the pen shell populations the  
438 occurrence of resistant individuals may be a major asset. Usually, large, adult individuals  
439 surviving two waves of the parasitic disease caused by *H. pinnae* do not die during further  
440 exposure (Vázquez-Luis, pers. comm.). Currently, only one living adult has been observed in  
441 the outer impacted area of Alfacs Bay (Prado, pers. observ.), which is consistent with mortality  
442 patterns close to 100% of individuals in other regions (Vázquez-Luis et al., 2017). Yet, 36  
443 surviving young specimens of reproductive age (ca. 30 cm; from 2017 recruitment) were  
444 observed in January 2020 in only 1 Ha within the most impacted area, and the presence of  
445 further numbers in adjacent sites needs to be explored. The cause of such higher survival in  
446 young specimens vs. adult individuals (35.6 and 0%, respectively) is unclear, although  
447 differences in the expression of immune genes and in the capacity to mitigate oxidative  
448 damage to support physiological functions have been observed over the lifetime of bivalves  
449 (Philipp and Abele, 2008; Husmann et al., 2014). Unfortunately, individuals might end dying if  
450 exposure to the pathogen persists throughout the growth period, as observed in later  
451 monitoring (77.78% found dead by May 2020; only 8 of the 36 young specimens were found

452 alive in late July), suggesting a narrow window of time for reproductive success to perpetuate  
453 the species. Also possibly, the abundance of *Mycobacterium* sp. might accumulate in larger  
454 individuals (A. Grau et al., unpublished data) and could contribute to increased mortality with  
455 age and explain observed patterns over time. Yet, apparently healthy young individuals  
456 showed presence of *Mycobacterium* sp. linked to strong inflammatory lesions in different  
457 Croatian regions affected by MMEs (Šarić et al., 2020). In fact, animal immune response to  
458 intracellular *Mycobacteria* spp. is complex, due to interaction between bacterial virulence and  
459 host resistance, two distinct and independent variables, leading to periods of remission  
460 followed with disease progression (Davidovich et al. 2020). In Alfacs Bay, *Mycobacterium* sp.  
461 was found in animals from the outer region closer to the mouth of the bay (coupled with *H.*  
462 *pinnae*; see also Carella et al., 2020), but not in middle and inner areas, suggesting that it could  
463 be even more sensitive than *H. pinnae* to salinity variations occurring in estuarine waters. In  
464 fact, *Mycobacterium* sp. has not been found in the Mar Menor lagoon either where salinities  
465 above those of the open sea are a common feature (Nebot-Colomer et al., submitted).

466 In Fangar Bay, where no positives have been found for *H. pinnae* or *Mycobacterium* sp., the  
467 salinity range to which the local population of *P. nobilis* is exposed is even lower, with an  
468 annual mean of ca. 32.4 (from ca. 27 to 36 during some winter months with low rainfall). In  
469 particular, salinities from ca. 30.5 to 33.5 were detected during the summer months (2018 and  
470 2019) with higher risk of disease, confirming that this might be a safe range to prevent  
471 infection by these pathogens (Cabanelas-Reboredo et al., 2019). Unfortunately, the availability  
472 of populations that exist in habitats with salinities consistently below the lower limit for the  
473 parasite (at 36.5) is, to our knowledge, very scarce. One possibility is the Sea of Marmara,  
474 where healthy populations are still found, possibly due to low salinities resulting from the  
475 mixing of Black Sea (ca. 18) and Aegean Sea waters (ca. 38.5) (Öndes et al., 2020), but more  
476 information is necessary about the species' abundance and seasonal fluctuations in salinities.  
477 Another example of a parasite-free area in the long-term could be the large pen shell

478 population in the Venice lagoon (Russo 2017), which appears to be exposed to annual salinity  
479 ranges of ca. 32-34 (Zirino et al., 2014). Similarly, there are also few examples such as that of  
480 the Mar Menor in Spain (usually 42 to 47; Fernández-Torquemada and Sánchez-Lizaso, 2011;  
481 Giménez-Casalduero et al., 2020) that are usually above the upper limit of salinity acceptable  
482 for distribution of the parasite, at 39. Even so, exceptional weather events bringing large  
483 amounts of rain into the lagoon were able to decrease salinity levels to ca. 39 and might have  
484 allowed the entrance of the parasite (Vázquez-Luis, pers. comm.), although no MMEs have yet  
485 been detected and the evolution of the disease is yet to be seen (Giménez-Casalduero, pers.  
486 comm.). Other populations inhabiting areas with a wider salinity range such as that of the Ghar  
487 El Melh lagoon in Tunisia (36 to 51; Zakhama-Sraieb et al., 2011) may also be presumably  
488 exposed to low risk due to lower salinity levels occurring during the winter period, when  
489 temperatures are less favorable for disease transmission (García-March et al., 2020a).

490 Although pen shell populations in confined waters appear to have a higher tolerance to  
491 disease that could help the species chances of surviving, these environments are also more  
492 vulnerable to severe weather phenomena. Twenty days after Storm Gloria, a MME of ca. 60%  
493 of the population, equally affecting young specimens and adult individuals, was observed in  
494 Fangar Bay. Gloria featured wave heights of up to 8 m along the Spanish Mediterranean coast,  
495 and in the Ebro Delta, which caused a major storm surge that entered 3 km inland, devastating  
496 rice paddies and coastal features (Amores et al., 2020). The event, however, did not cause any  
497 dislodgement of pen shells within Alfacs or Fangar Bays. This suggests that despite  
498 hydrodynamic conditions these habitats may have a major structuring role in pen shell  
499 populations (García-March et al., 2007a; Hendricks et al., 2011), as both locations are  
500 effectively protected from wind-waves. In contrast, rain induced flooding decreased the  
501 salinity of Fangar Bay to values around 11 during an approximate period of 10 days.  
502 Comparatively, these salinity values are much lower than those observed in Alfacs Bay  
503 (approximately 32) where the surface area is ca. 4 times the size and therefore attaining lower

504 dilution from rainfall. To our knowledge, this is the first time that the species is reported to be  
505 exposed to such a low salinity within such a short period following heavy rain. Hernandis et al.  
506 (2018), studied salinity variations in three different areas of Boka Kotorska Bay (Montenegro),  
507 and found decreases down to ca. 19 following punctual but high inputs of freshwater with no  
508 apparent effect on pen shell populations, although the exact duration of the effect is unknown  
509 (measures conducted every two weeks). Also possibly, the influence of wave action on the  
510 resuspension of fine sediments may have further contributed to observed effects. Episodes of  
511 strong weather have been shown to cause large sediment fluctuations and *in situ* burial of  
512 cockle (Dare 2004) and mussel beds even at high biomasses of mussels (Landahl 1988).  
513 Further, storms have been identified as a major factor limiting the distribution of mussel beds  
514 to sheltered areas of the coast due to scarcity of phytoplankton and competition for food with  
515 other communities of filter feeders (Nehls and Thiel 1993). In Fangar Bay, pen shells are  
516 located on a shallow seagrass bed of *C. nodosa*, which might have prevented burial by a  
517 sediment layer. However, our measures of water transparency from the Secchi disc and  
518 satellite images (ICGC visor) demonstrate increased turbidity in the water column over an  
519 estimated time period of around 10 days. Later in March, a further decrease in water  
520 transparency was also observed, coinciding with pumping of seawater from flooded rice  
521 drainage channels into Fangar Bay (see <http://www.saihebro.com>), which might have hindered  
522 the recovery of the remaining pen shells and contributed to additional mortalities. Pen shells  
523 have been shown to filter small-size sediment particles (< 200 µm) without an apparent  
524 assimilation for tissue growth (Prado et al., 2020b), thus suggesting a reduced intake during  
525 the siltation period. In other species such as the green-lipped mussel *Perna viridis*,  
526 experimental exposure to high loads of suspended solids caused no direct mortality during a  
527 period of 96 h (much shorter than Storm Gloria effects), although serious damage was  
528 reported in the structure of the gills that may impair long-term feeding and respiration (Shin et  
529 al., 2002). There may also have been some feeding and metabolic impairment as also

530 suggested by the histological examination of the gonads of the 3 individuals sacrificed after  
531 Storm Gloria, in which there were found few oocytes attached to the developing gonadal  
532 follicle as described for the post-reproductive period in late summer (Prado et al., 2020a;  
533 Deudero et al., 2017). This gonad regression observed 20 days after the storm was very likely a  
534 symptom of discomfort and physiological impairment, which ended with the death of nearly  
535 100% of the population (only 12 individuals were found alive in early March 2020) about 1.5  
536 months later.

537 Our results for the age structure of the population show that most of the individuals were  
538 young; the oldest were in the range of 4 to 7 years (much younger than the Alfacs Bay) and  
539 featured an  $L_{\infty}$  of 41.9 suggesting that the baseline conditions of the population were already  
540 stressing and individuals might have reduced tolerance to additional distress. Such reduced  
541 life-expectancy and maximum size compared to other Mediterranean populations reaching  
542 over 50 years of age (Rouanet et al., 2015) and greater maximum sizes (García-March et al.,  
543 2020b) demonstrate that pen shells in Fangar Bay are subjected to extremely harsh conditions,  
544 -reduced salinity and desiccation at shallow depth-, causing continuous shell fractures and  
545 reconstructions. Yet, the area also hosted numerous old shells remains (approx. 500),  
546 indicating that the species may have dwelled for decades in Fangar Bay. The results indicate  
547 there has been some recruitment for most of the years (60 young specimens of 2-3 years old,  
548 and shells of 4 to 7 years), and although the effect of external supply cannot be discarded due  
549 to the presence of healthy populations in the southern French Mediterranean coast until mid-  
550 2018 (García-March et al., 2020a), the histological results indicate that the population was  
551 fertile. Now, unless self-recruitment occurs among the few individuals that are still alive or  
552 some managerial intervention is conducted with healthy individuals from Alfacs Bay, the  
553 population may face extinction in just 2-3 years. Seasonal monitoring is also needed to assess  
554 potential (although improbable) recruitment, particularly in zone 1 where an even shallower  
555 bathymetry acts as a physical barrier favoring larval settlement while hampering long-term

556 growth (only three adults were found in this zone in February 2020; see also Prado et al.,  
557 2020a for similar patterns in Alfacs Bay), thus this population will also require later  
558 translocation of individuals.

559

## 560 **5. Conclusions**

561 The Fangar population subjected to salinities of 30.5 to 33.5 during the summer period  
562 appears to be in a safe range to avoid the entrance of the pathogens (both *H. pinnae* and  
563 *Mycobacterium* sp.), but pen shells are rarely found in these extreme conditions. Most of the  
564 remaining populations in confined waters fall outside the 36.5 to 39 salinity range during some  
565 annual periods and are less vulnerable (Cabanellas-Reboredo et al., 2019), but not protected  
566 against infection by *H. pinnae* as evidenced for the Alfacs Bay population. Aside the degree of  
567 connection with the open sea, the chances of infection and the evolution of MMEs appear to  
568 be related to the time gap that populations are exposed to favorable salinities for the parasite  
569 and its interaction with seasonal temperatures. In Alfacs Bay, attaining even slightly lower  
570 salinities during the hottest summer months could be a feasible goal that could be  
571 accomplished thanks to the availability of a major network of drainage channels for rice  
572 agriculture that may enhance freshwater release, and help to minimize the spread of the  
573 parasite. Populations in confined waters may be more exposed to changes in environmental  
574 conditions compared to the open sea and are more vulnerable to severe weather phenomena  
575 (Fangar Bay, this study) or increased eutrophication (Mar Menor; García-Ayllon, 2018).  
576 According to historic data, 30 river floods greater than 2000 m<sup>3</sup>/s have occurred in the Ebro  
577 Delta from 1779 to 2001, with years registering up to 3 storms and gap periods of over 20  
578 years (DMAH, 2008). Therefore, although this might constrict the establishment of a  
579 permanent population in Fangar Bay, it should still provide a more secure environment than  
580 the open sea in the context of the present pandemics.



581 Urgent actions are necessary to manage the salinity and conditions of habitat quality of  
582 these last remaining populations to prevent, as much as possible, further losses of individuals.  
583 Moreover, immunological studies (*in vitro* and *in vivo*) are needed to evaluate pen shells  
584 response to pathogens along the salinity gradient. Suboptimal salinity conditions can result in  
585 changes in bivalve defense mechanisms, growth, oxygen consumption, heart and filtration rate  
586 (Matozzo and Marin, 2011) that act on many aspects of disease pathogenesis. The knowledge  
587 of the mechanisms involved in immune modulation is crucial to develop management and  
588 conservation programs. The finding and preservation of surviving individuals (preferably adults  
589 but also young specimens) is another critical goal requiring intervention, rather than left to  
590 chance.

591

#### 592 **Acknowledgements**

593 Authors would like to thank the Ministry for the Ecological Transition and the Demographic  
594 challenge for supporting a part of the work through the PinnaSpat project with the Biodiversity  
595 Foundation. Further funding for monthly monitoring in the Alfacs Bay was provided by the  
596 Service of Fauna and Flora of the Catalonia Government (Ref: PTOP/CP00034 PTOP-2019-404).  
597 P Prado and G Catanese were contracted under the INIA-CCAA cooperative research program  
598 for postdoctoral incorporation from the Spanish National Institute for Agricultural and Food  
599 Research and Technology (INIA), with additional support from project EMERGER (E-RTA2015-  
600 00004-00-00). Authors would like to thank Carles Alcaraz for statistical advice, and José Luis  
601 Costa and David Mateu for technical assistance during fieldwork sampling.

602

603

604 **References**

- 605 Addis, P., Secci, M., Brundu, G., Manunza, A., Corrias, S., Cau, A., 2009. Density, size structure,  
606 shell orientation and epibiotic colonization of the fan mussel *Pinna nobilis* L. 1758  
607 (Mollusca: Bivalvia) in three contrasting habitats in an estuarine area of Sardinia (W  
608 Mediterranean). *Sci. Mar.* 73, 143-152.
- 609 Amores, A., Marcos, M., Carrió, D. S., Gómez-Pujol, L., 2020. Coastal Impacts of Storm Gloria  
610 (January 2020) over the Northwestern Mediterranean, *Nat. Hazards Earth Syst. Sci.* 20,  
611 1955–1968.
- 612 Belando, M. D., García-Muñoz, R., Ramos, A., Franco, I., Bernardeau-Esteller, J., García, P., Ruiz,  
613 J. M., 2015. Distribution and abundance of *Cymodocea nodosa* meadows and *Pinna nobilis*  
614 populations in the Mar Menor coastal lagoon (Murcia, South East of Spain). *PeerJ PrePrints*.
- 615 Böddinghaus, B., Rogall, T., Flohr, T., Blöcker, H., Böttger, E.C. ,1990. Detection and  
616 identification of mycobacteria by amplification of rRNA. *J. Clin. Microbiol.* 28, 1751–1759.
- 617 Cabanellas-Reboredo, M., Vázquez-Luis, M., Mourre, B., et al., 2019. Tracking the mass  
618 mortality outbreak of pen shell *Pinna nobilis* populations: a collaborative effort of scientists  
619 and citizens. *Sci. Rep.* 9, 13355.
- 620 Carella, F., Elisabetta, A., Simone, F., Fulvio, S., Daniela, M., Prado, P., Rosella, P., Marino, F.,  
621 Eleonora, F., Tobia, P., De Vico, G., 2020. In the wake of the ongoing mass mortality events:  
622 Co-occurrence of Mycobacterium, Haplosporidium and other pathogens in *Pinna nobilis*  
623 collected in Italy and Spain (Mediterranean Sea). *Front. Mar. Sci* 7, 48.
- 624 Carella, F., Aceto, S., Pollaro, G., Micccio A., Carrasco N., Prado P., De Vico, G., 2019. An  
625 emerging mycobacterial disease is associated with the silent mass mortality of the Pen shell  
626 *Pinna nobilis* along Tyrrhenian coastline of Italy. *Sci. Rep.* 9, 2725.
- 627 Catanese, G., Grau, A., Valencia, J.M., Garcia-March, J.R., Vázquez-Luis, M., Alvarez, E.,  
628 Deudero, S., Darriba, S., Carballal, M.J., Villalba, A., 2018. *Haplosporidium pinnae* sp. nov., a

629 haplosporidan parasite associated with mass mortalities of the fan mussel, *Pinna nobilis*, in  
630 the Western Mediterranean Sea. J. Invert. Pathol. 157, 9–24.

631 Cerralbo, P., Espino, M., Grifoll, M., Valle-Levinson, A., 2019. Subtidal circulation in a microtidal  
632 Mediterranean bay. Sci. Mar. 82(4), 231–243.

633 Coppa, S., de Lucia, G. A., Magni, P., Domenici, P., Antognarelli, F., Satta, A., Cucco, A., 2013.  
634 The effect of hydrodynamics on shell orientation and population density of *Pinna nobilis* in  
635 the Gulf of Oristano (Sardinia, Italy). J. Sea Res. 76, 201-210.

636 Dare, P.J., Bell, M.C., Walker, P., Bannister, R.C.A., 2004. Historical and current status of cockle  
637 and mussel stocks in The Wash. CEFAS, Lowestoft, 85.

638 Davidovich N., Morick D., Carella F., 2020. Mycobacteriosis in aquatic invertebrates: A review  
639 of its emergence. Microorganisms 8(8), 1249.

640 De Gaulejac, B., 1995. Mise en évidence de l’hermaphrodisme successif à maturation  
641 asynchrone de *Pinna nobilis* (L.) (Bivalvia: Pterioidea). Comptes rendus de l’Académie des  
642 Sciences, Série 3, Sci. Vie 318, 99-103.

643 Delgado, M., 1987. Fitoplancton de las bahías del Delta del Ebro. Inv. Pesq. 51, 517-548.

644 Deudero, S., Grau, A., Vázquez-Luis, M., Álvarez, E., Alomar, C., Hendriks, I.E., 2017.  
645 Reproductive investment of the pen shell *Pinna nobilis* Linnaeus, 1758 in Cabrera National  
646 Park (Spain). Medit. Mar. Sci. 18, 271–284.

647 DMAH, 2008. Series of framework studies for later use in defining a strategy for preventing  
648 and adapting to climate change in Catalonia, Framework Study N1: Ebro Delta. Department  
649 of Environment and Housing, Government of Catalonia, Barcelona.

650 Fernández-Torquemada, Y., Sánchez-Lizaso, J.L., 2011. Responses of two Mediterranean  
651 seagrasses to experimental changes in salinity. Hydrobiologia 669, 21.

652 Foulquié, M., Dupuy de la Grandrive, R., Dalias, N., Vicente, N., 2020. Inventory and health  
653 status of the populations of *Pinna nobilis* (L.1758) in Thau lagoon (Herault, France), 2020.  
654 Marinelifere-revue.fr, 1-25.

655 García-Ayllon, S., 2018. The Integrated Territorial Investment (ITI) of the Mar Menor as a  
656 model for the future in the comprehensive management of enclosed coastal seas. *Ocean*  
657 *Coast. Manag.* 166, 82–97.

658 García-March, J.R., Tena, J., Henandis, S., et al., 2020a. Can we save a marine species affected  
659 by a highly infective, highly lethal, waterborne disease from extinction?. *Biol. Conserv.* 243,  
660 108498.

661 García-March, J. R., Hernandis, S., Vázquez-Luis, M., Prado, P., Deudero, S., Vicente, N., Tena-  
662 Medialdea, J., 2020b. Age and growth of the endangered fan mussel *Pinna nobilis* in the  
663 western Mediterranean Sea. *Mar. Environ. Res.* 153, 104795.

664 García-March, J.R., A. Marquez-Aliaga, Y.G. Wang, D. Surge, Kersting, D.K., 2011. Study of *Pinna*  
665 *nobilis* growth from inner record: how biased are posterior adductor muscle scars  
666 estimates? *J. Exp. Mar. Biol.Ecol.* 407, 337–344.

667 García-March, J.R., Pérez-Rojas, L., García-Carrascosa, A.M. 2007a. Influence of hydrodynamic  
668 forces on population structure of *Pinna nobilis* L., 1758 (Mollusca: Bivalvia): The critical  
669 combination of drag force, water depth, shell size and orientation. *J. Exp. Mar. Biol.Ecol.*  
670 342(2), 202-212.

671 García-March, J.R., García-Carrascosa, A.M., Cantero, A.P., Wang, Y.G., 2007b. Population  
672 structure, mortality and growth of *Pinna nobilis* Linnaeus, 1758 (Mollusca, Bivalvia) at  
673 different depths in Moraira bay (Alicante, Western Mediterranean). *Mar. Biol.* 150(5), 861-  
674 871.

675 García-March, J. R., Márquez-Aliaga, A., 2007. *Pinna nobilis* L., 1758 age determination by  
676 internal shell register. *Mar. Biol.* 151: 1077–1085.

677 García-Pintado, J., Martínez-Mena, M., Barberá, G.G., Albaladejo, J., Castillo, V.M., 2007.  
678 Anthropogenic nutrient sources and loads from a Mediterranean catchment into a coastal  
679 lagoon: Mar Menor, Spain. *Sci. Tot. Environ.* 373(1), 220-239.

680 Giménez-Casalduero, F., Gomariz-Castillo, F., Alonso-Sarría, F., Cortés, E., Izquierdo-Muñoz, A.,  
681 Ramos, A., 2020. *Pinna nobilis* in the Mar Menor coastal lagoon: a story of colonization and  
682 uncertainty. Mar. Ecol. Progr. Ser. 652, 77–94.

683 Guallart, J., Templado, J. 2012. *Pinna nobilis*. In: VV.AA., Bases ecológicas preliminares para la  
684 conservación de las especies de interés comunitario en España: Invertebrados.  
685 Ministerio de Agricultura, Alimentación y Medio Ambiente, Madrid.

686 Hendriks, I.E., Cabanellas-Reboredo, M., Bouma, T.J., Deudero, S., Duarte, C.M., 2011. Seagrass  
687 meadows modify drag forces on the shell of the fan mussel *Pinna nobilis*. Estuar. Coasts  
688 34(1), 60-67.

689 Husmann, G., Abele, D., Rosenstiel, P., Clark, M.S., Kraemer, L., Philipp, E.E.R., 2014. Age-  
690 dependent expression of stress and antimicrobial genes in the hemocytes and siphon tissue  
691 of the Antarctic bivalve, *Laternula elliptica*, exposed to injury and starvation. Cell Stress  
692 Chap. 19(1), 15-32.

693 Hernandis, S., Joksimović, D., Tena, J., Vicente, N., Mačić, V., García-March, J.R., Castelli, A.,  
694 Torres, J., Mitrić, M., Martinović, R., 2018. Comparison of habitat structure of 4 dense  
695 populations of the critically endangered fan mussel (*Pinna nobilis*). Int. Symp. Mar. Sci. Book  
696 of abstracts.

697 Isla, F.I., 2009. Coastal lagoons. Coastal zones and estuaries, 320-338.

698 Katsanevakis, S., 2007. Growth and mortality rates of the fan mussel *Pinna nobilis* in Lake  
699 Vouliagmeni (Korinthiakos Gulf, Greece): a generalized additive modelling approach.  
700 Mar. Biol. 152, 1319–1331.

701 Kersting, D., Benabdi, M., Čížmek, H., Grau, A., Jimenez, C., Katsanevakis, S., Öztürk, B., Tuncer,  
702 S., Tunesi, L., Vázquez-Luis, M., Vicente, N. Otero Villanueva, M., 2019. *Pinna nobilis*. The  
703 IUCN Red List of Threatened Species 2019: e.T160075998A160081499.  
704 <https://dx.doi.org/10.2305/IUCN.UK.2019-3.RLTS.T160075998A160081499.en>.

705 Downloaded on 23 February 2020.

706 Landahl, J., 1988. Sediment-level fluctuation in a mussel bed on a 'protected' sand-gravel  
707 beach. *Estuar. Coast. Shelf Sci.* 26, 255-267.

708 Lattos, A., Giantsis, I. A., Karagiannis, D., Michaelidis, B., 2020. First detection of the invasive  
709 Haplosporidian and Mycobacteria parasites hosting the endangered bivalve *Pinna nobilis* in  
710 Thermaikos Gulf, North Greece. *Mar. Environ. Res.*, 155, 104889.

711 Llebot, C., Solé, J., Delgado, M. Fernández-Tejedor, M., Camp, J., Estrada, M., 2011.  
712 Hydrographical forcing and phytoplankton variability in two semi-enclosed estuarine bays.  
713 *J. Mar. Syst.* 86, 69–86.

714 López-Sanmartín, M., Catanese, G., Grau, A., Valencia, J. M., García-March, J. R., Navas, J. I.,  
715 2019. Real-Time PCR based test for the early diagnosis of *Haplosporidium pinnae* affecting  
716 fan mussel *Pinna nobilis*. *PLoS one*, 14, e0212028.

717 Matozzo, V., Marin, M. G., 2011. Bivalve immune responses and climate changes: is there a  
718 relationship?. *Invert. Surviv. J.* 8, 70-77.

719 Nebot-Colomer, E., Belando, M. D., Deudero, S., Catanese, G., Esteller, J. B., García Muñoz, R.,  
720 Ramos Segura, A., Ruiz, J. M., Vázquez-Luis, M., submitted. Will one of the last *Pinna nobilis*  
721 populations survive inhabiting in a eutrophicated coastal lagoon with a new emerging  
722 threat? *Aquat. Conser.: Mar. Freshw. Ecosyst.*

723 Nehls, G. Thiel, M., 1993. Large-scale distribution patterns of the mussel *Mytilus edulis* in the  
724 Wadden Sea of Schleswig-Holstein: do storms structure the ecosystem? *Neth. J. Sea Res.*,  
725 31, 181-187.

726 Philipp, E.E.R., Abele, D., 2010. Masters of longevity: lessons from long-lived bivalves—a mini-  
727 review. *Gerontology* 56(1), 55–65.

728 Öndes, F., Alan, V., Akçalı, B., Güçlüsoy, H., 2020. Mass mortality of the fan mussel, *Pinna*  
729 *nobilis* in Turkey (eastern Mediterranean). *Mar. Ecol.*, e12607.

730 Prado, P., Andree, K. B., Trigos, S., Carrasco, N., Caiola, N., García-March, J.R., Tena, J.,  
731 Fernández-Tejedor, M., Carella, F., 2020a. Breeding, planktonic and settlement factors

732 shape recruitment patterns of one of the last remaining major population of *Pinna nobilis*  
733 within Spanish waters. *Hydrobiologia* 847, 771-786.

734 Prado, P., Cabanes, P., Catanese, G., Carella, F., Carrasco, N., Grau, A., Hernandis, S., García-  
735 March, J.R., Tena, J., Andree, K.B., 2020b. Growth of juvenile *Pinna nobilis* in captivity  
736 conditions: Dietary and pathological constraints. *Aquaculture*, 735167.

737 Prado, P. 2018. Seagrass epiphytic assemblages are strong indicators of agricultural discharge  
738 but weak indicators of host features. *Estuar. Coast. Shelf Sci.* 204, 140-148.

739 Prado, P., Caiola, N., Ibáñez, C., 2014. Habitat use by a large population of *Pinna nobilis* in  
740 shallow waters. *Sci. Mar.* 78, 555-565.

741 Quijano-Scheggia, S., Garcés, E., Flo, E., Fernandez-Tejedor, M., Diogène, J., Camp, J., 2008.  
742 Bloom dynamics of the genus *Pseudo-nitzschia* (Bacillariophyceae) in two coastal bays (NW  
743 Mediterranean Sea). *Sci. Mar.* 72, 577-590.

744 Rouanet, E., Trigos, S., Vicente, N., 2015. From youth to dead of old age: the 50-year story of a  
745 *Pinna nobilis* fan mussel population at Port-Cros Island (Port-Cros National Park, Provence,  
746 Mediterranean Sea). *Sci. Reports Port-Cros Natl. Park*, 29, 209-222.

747 Russo, P., 2017. Lagoon malacofauna: results of malacological research in the Venice Lagoon.  
748 *Bollet. Malacol.* 53, 49-62.

749 Šarić T., Župan I., Aceto S., Villari G., Palić D., De Vico G., Carella F., 2020. Epidemiology of  
750 noble pen shell (*Pinna nobilis* L. 1758): Mass mortality events in Adriatic Sea is  
751 characterized with rapid spreading and acute disease progression. *Pathogens.* 9(10), 776.

752 Shin, P.K.S., Yau, F.N., Chow, S.H., Tai, K.K., Cheung, S.G., 2002. Responses of the green-lipped  
753 mussel *Perna viridis* (L.) to suspended solids. *Mar. Poll. Bull.* 45, 157-162.

754 Simide, R., Couvray, S. Vicente, N., 2019. Présence de *Pinna nobilis* (L. 1758) dans l'étang  
755 littoral de Diana (Corse). *Mar. Life Rev.*, 1-4.

756 Underwood, A.J., 1997. Experiments in ecology: their logical design and interpretation using  
757 analysis of variance. Cambridge University Press, Cambridge.

758 Vázquez-Luis, M., Álvarez, E., Barraón, A., García-March, J. R., et al., 2017. SOS *Pinna nobilis*: a  
759 mass mortality event in western Mediterranean Sea. *Front. Mar. Sci.* 4, 220.

760 Wesselmann, M., González-Wangüemert, M., Serrão, E. A. et al., 2018. Genetic and  
761 oceanographic tools reveal high population connectivity and diversity in the endangered  
762 pen shell *Pinna nobilis*. *Sci. Rep.* 8, 1-11.

763 Zakhama-Sraieb R., Sghaier Y.R., Omrane A., Charfi-Cheikhrouha, F., 2011. Density and  
764 population structure of *Pinna nobilis* (Mollusca, Bivalvia) in the Ghar El Melh lagoon (N-E  
765 Tunisia). *Bull. Inst. Natn. Scien. Tech. Mer de Salammbô* 38, 65-71.

766 Zirino, A., Elwany, H., Neira, C., Maico, F., Mendoza, G., Levin, L.A., 2014. Salinity and its  
767 variability in the lagoon of Venice, 2000–2009. *Adv. Oceanogr. Limnol.* 5, 41–59.

768



769 **Fig. 1.** Map of the Ebro Delta showing the location of Alfacs Bay in the South and Fangar Bay in  
770 the North. A) In Fangar Bay, we indicate the four study zones where mortality patterns were  
771 assessed after Storm Gloria. Shallow seagrass beds along the four study area are indicated.  
772 Monitoring circles were deployed within zone 3, which had the highest abundance of  
773 individuals. B) In Alfacs Bay, the three study zones (Z1, Z2, and Z3) are indicated, as well as the  
774 1 ha adjacent to Z1 where an extensive search for surviving individuals was conducted.  
775

776 **Fig. 2.** Mortality patterns in Alfacs Bay. A) Cumulative mortality in monitoring circles located in  
777 the three study zones of Alfacs Bay, and (B) Abundance of living and dead individuals (adults  
778 and young specimens) in 1 ha of Alfacs Bay located within the mass mortality area next to the  
779 mouth of the bay (i.e., adjacent to Zone 1). DY= Dead Young specimens, LY= Living Young  
780 specimens, LA= Living Adults, DA= Dead Adults. Error bars are SE.  
781

782 **Fig. 3.** Mortality patterns in Fangar Bay. A) Cumulative mortality in the three monitoring circles  
783 within Zone 3, and B) abundance of living and recently dead individuals (also young specimens  
784 and adults), and old shells in the four contiguous zones of Fangar Bay where the entire  
785 population is distributed. DY= Dead Young specimens, LY= Living Young specimens, LA= Living  
786 Adults, RDA= Recently Dead Adults; RDY= Recently Dead Young specimens, OS= Old Shells.  
787 Error bars are SE.  
788

789 **Fig. 4.** Age structure and year of recruitment of Fangar Bay population from shells (N = 20)  
790 collected on February 11<sup>th</sup> 2020. The presence of 60 young specimens too small to be aged  
791 using the dating technique (2-3 years age) is also indicated.  
792

793 **Fig. 5.** Histological sections of pen shell digestive gland and gonads from Fangar Bay after  
794 Storm Gloria. A) Section of the digestive gland at low magnification (20x) showing normal

795 digestive tubules (DT). B-C-) Higher magnification (40x) micrograph of the gonads, with acini  
796 full of regressing previtellogenic (B), and vitellogenic oocytes (C). In both cases, very few viable  
797 oocytes (OO) can be still observed attached to the developing follicle. Abundant hemocytes (\*)  
798 coupled with brown cells (BC) can be observed. A-C). H&E staining (for interpretation of the  
799 references to color in this figure legend, the reader is referred to the web version of this  
800 article).

801

802 **Fig. 6.** Variability in physicochemical variables across the study period (January 2018 to March  
803 2020) in the 3 zones of Alfacs Bay, and in Fangar Bay. A-B) Temperature (°C); C-D) Salinity; E-F)  
804 dissolved oxygen; and G-H) pH. Error bars are SE.

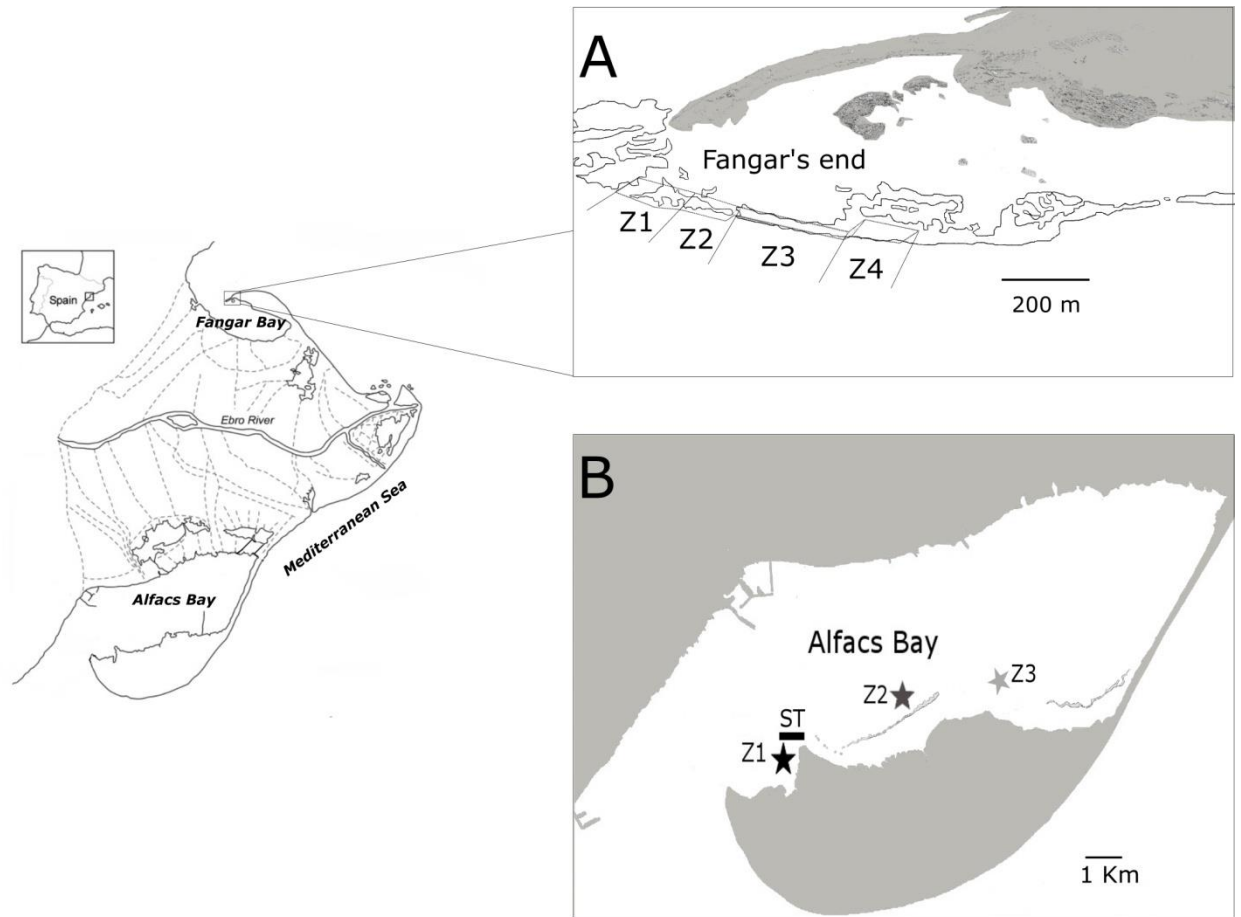
805

806 **Fig. 7.** Association between cumulative mortality rates in each zone and circle and salinity  
807 values in July-August 2018 and 2019. The significant  $R^2$  value and the line equation are  
808 indicated.

809

810 **Fig. 8.** Changes in FQ variables in Fangar Bay before and after Storm Gloria. A) Temperature  
811 (°C); B) salinity; C) dissolved oxygen (%); D) pH; E) Secchi disc visibility (m); F) Chlorophyll ( $\mu\text{g} \cdot$   
812  $\text{L}^{-1}$ ). The dotted lines indicate the dates of the mortality assessment on the 11<sup>th</sup> February 2020  
813 (individuals were found in an advanced stage of decomposition) and the 3<sup>rd</sup> of March 2020.  
814 Error bars are SE.

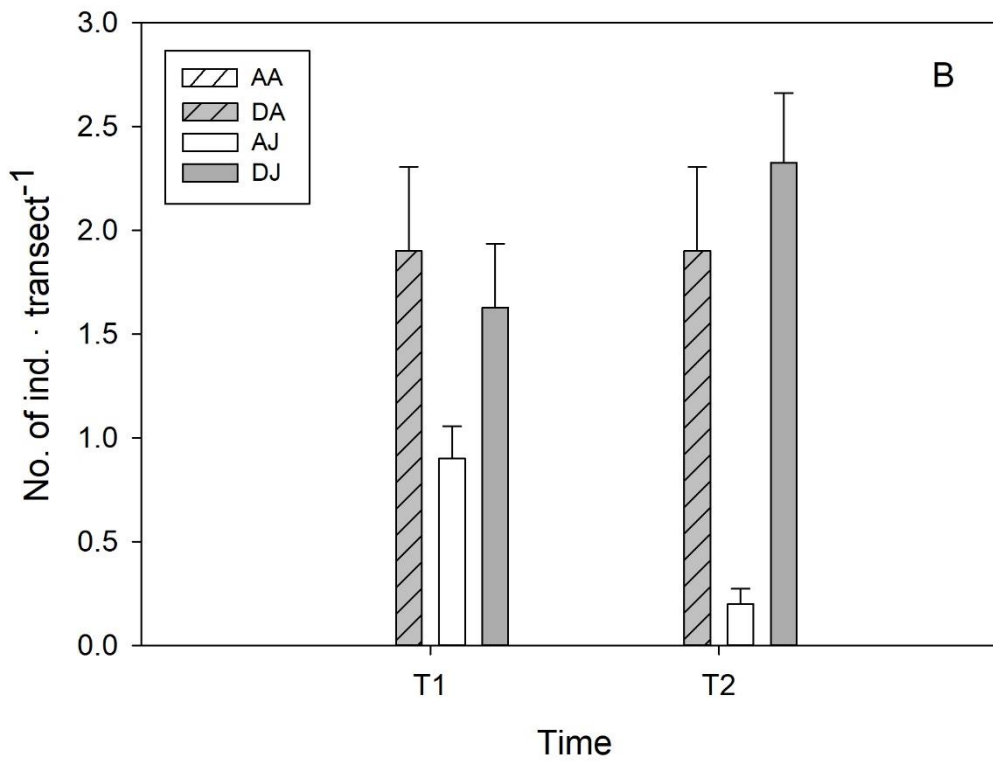
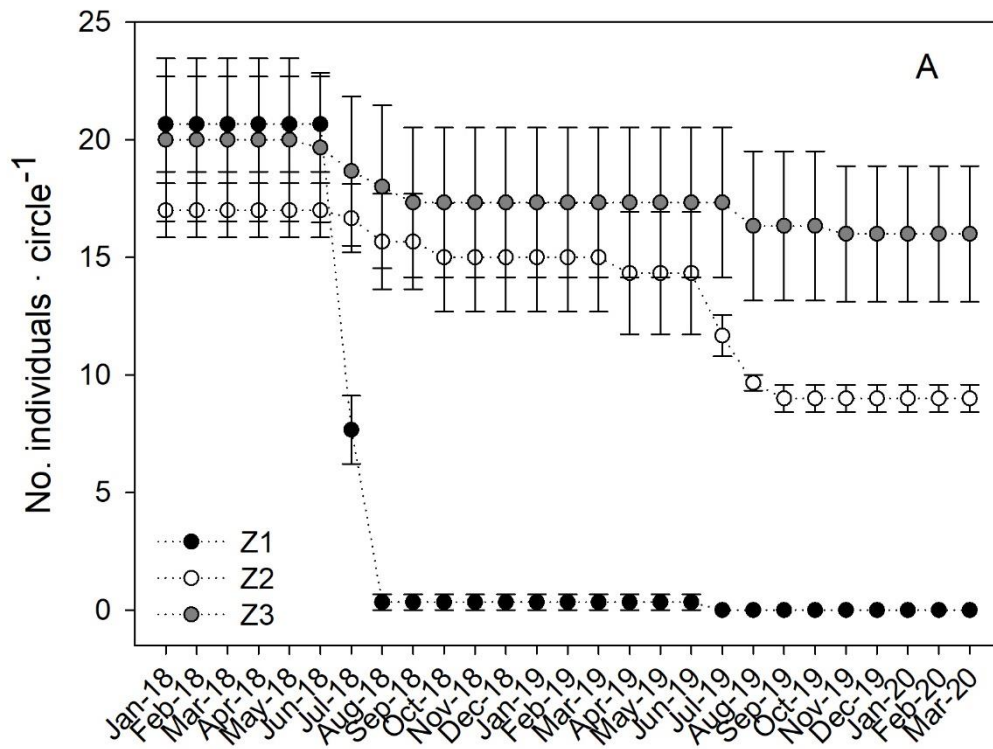
815



816

817 **Fig. 1**

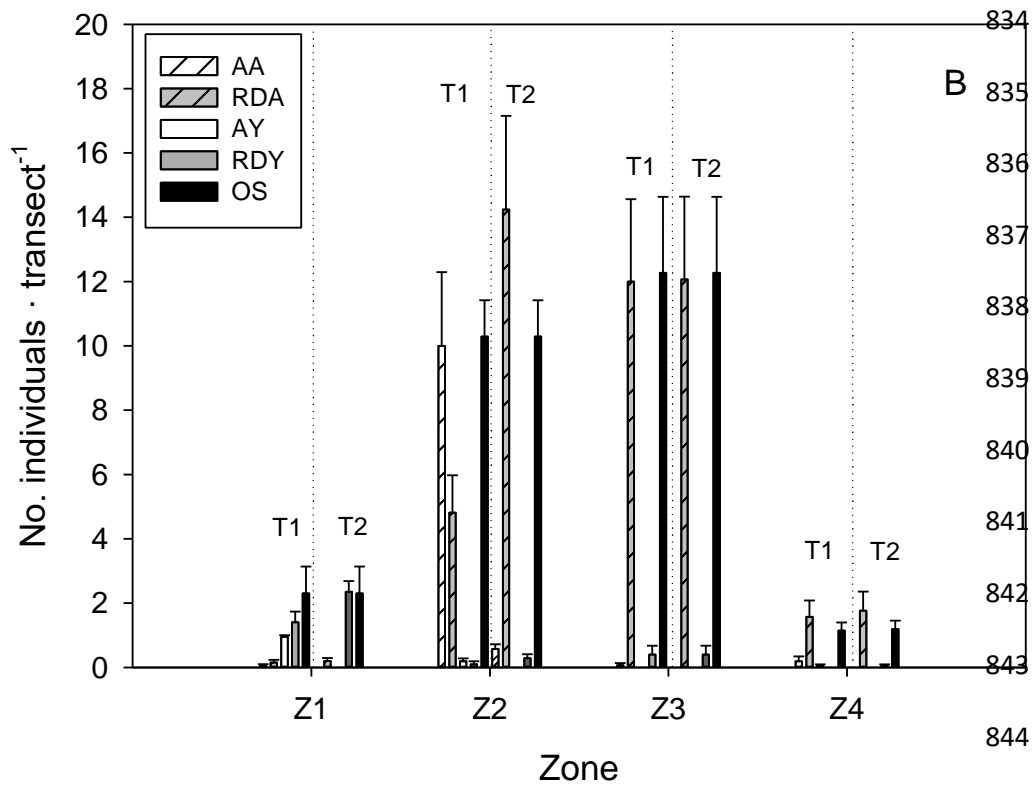
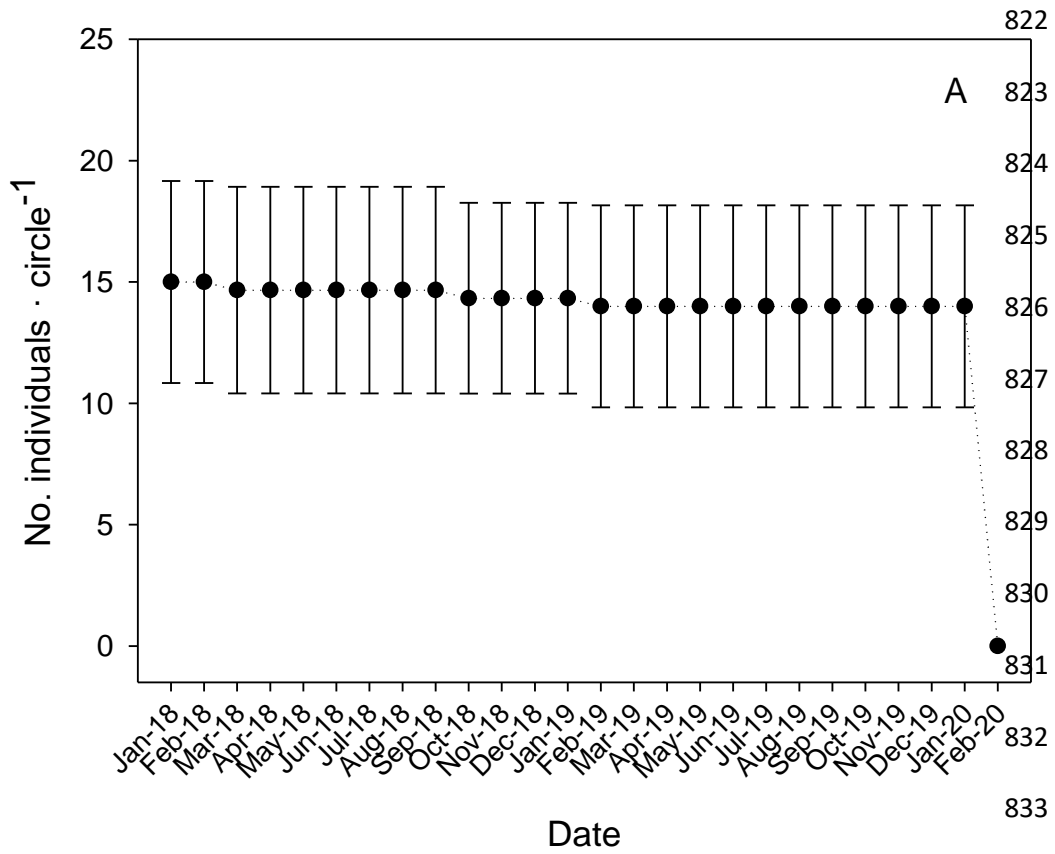
818



819

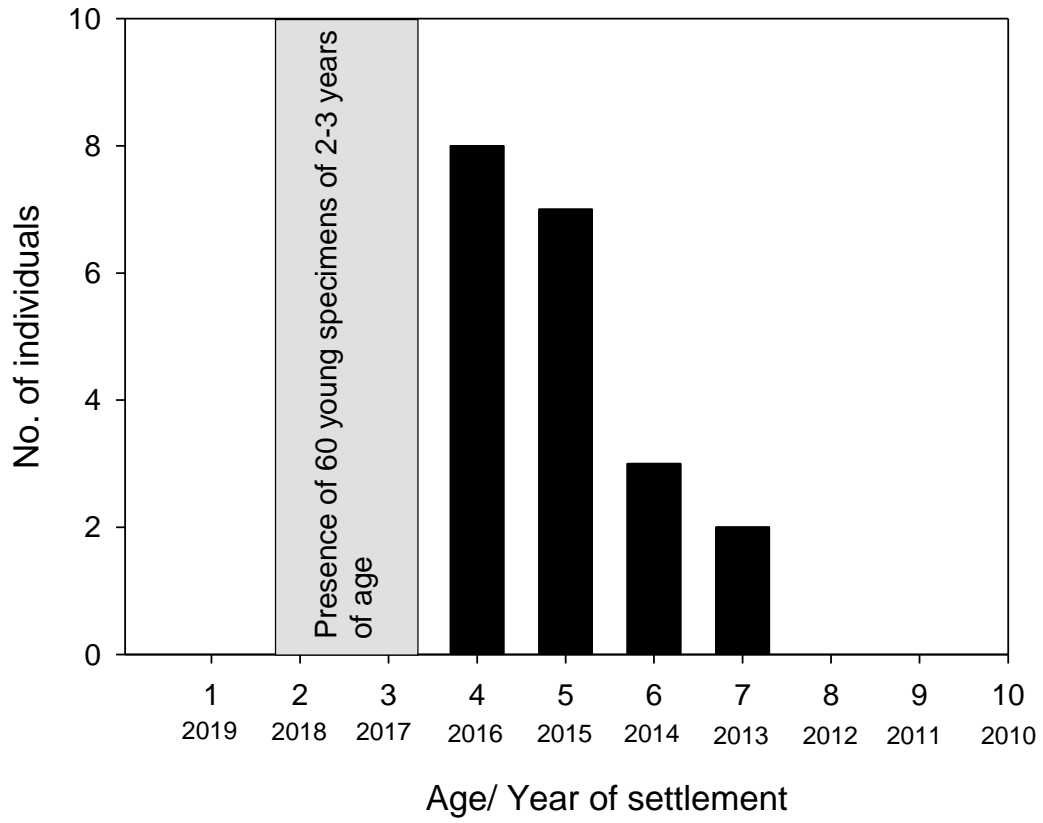
820 Fig. 2

821



845 Fig. 3

846



847

848

849 **Fig. 4**

850

851

852

853

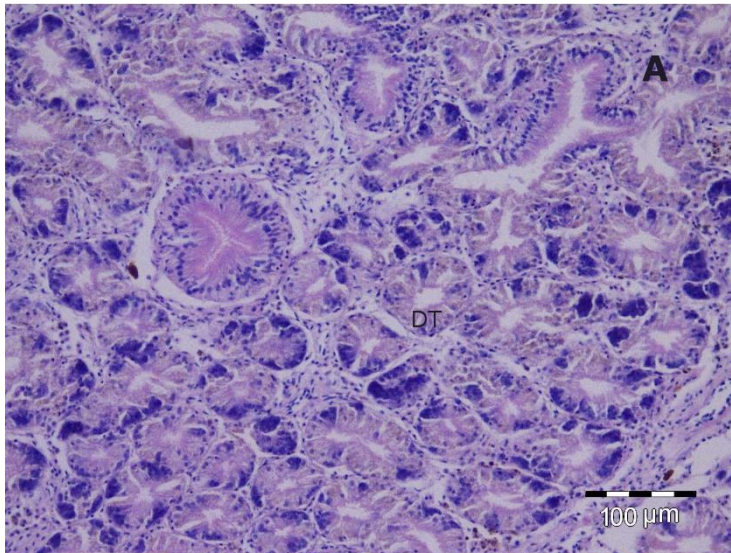
854

855

856

857

858



859

860

861

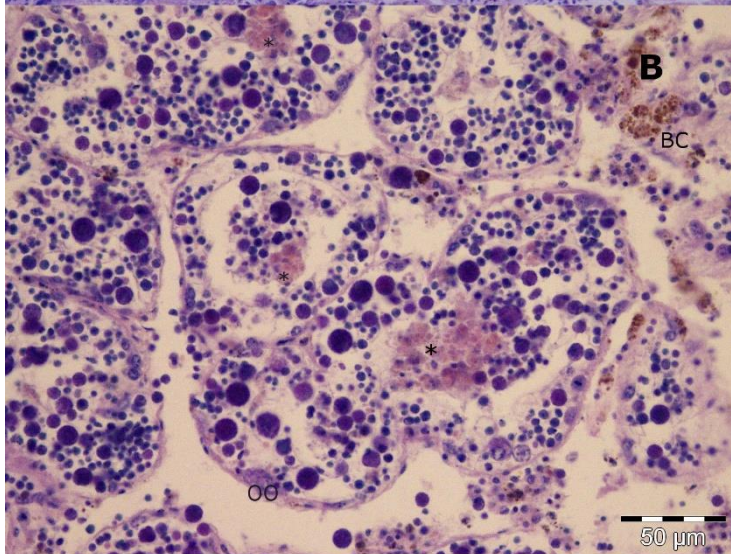
862

863

864

865

866



867

868

869

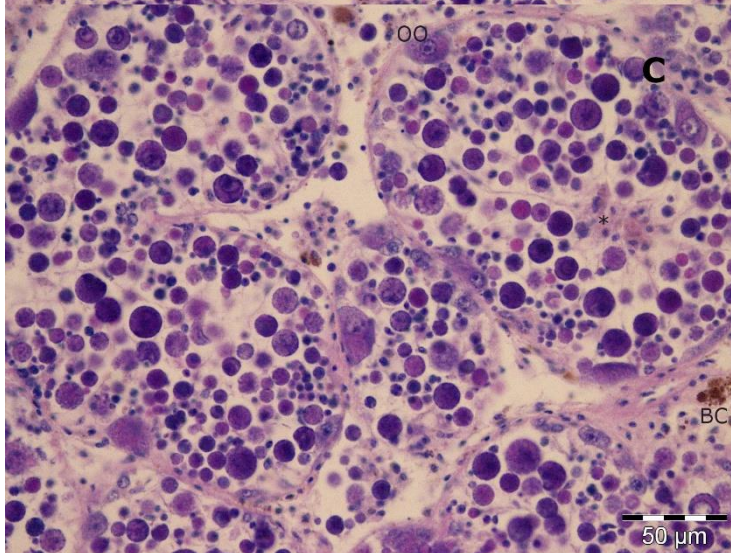
870

871

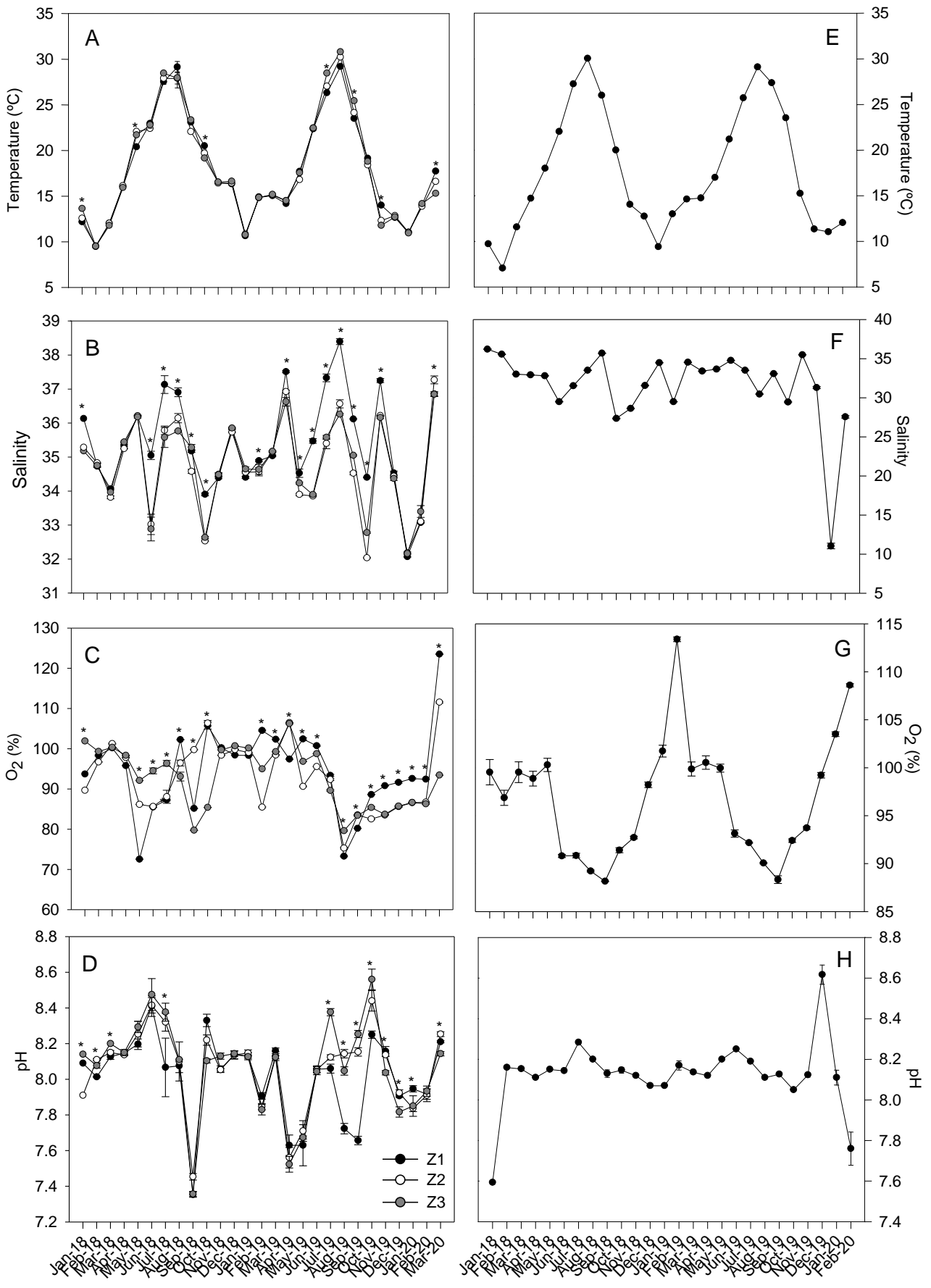
872

873

874

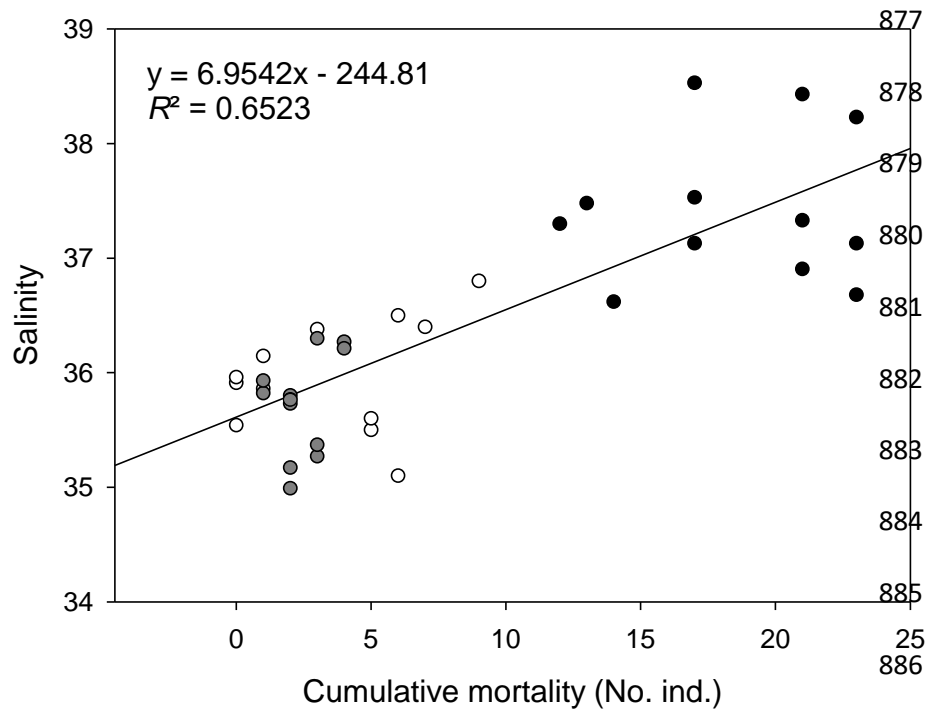


875 **Fig. 5**



876 Fig. 6

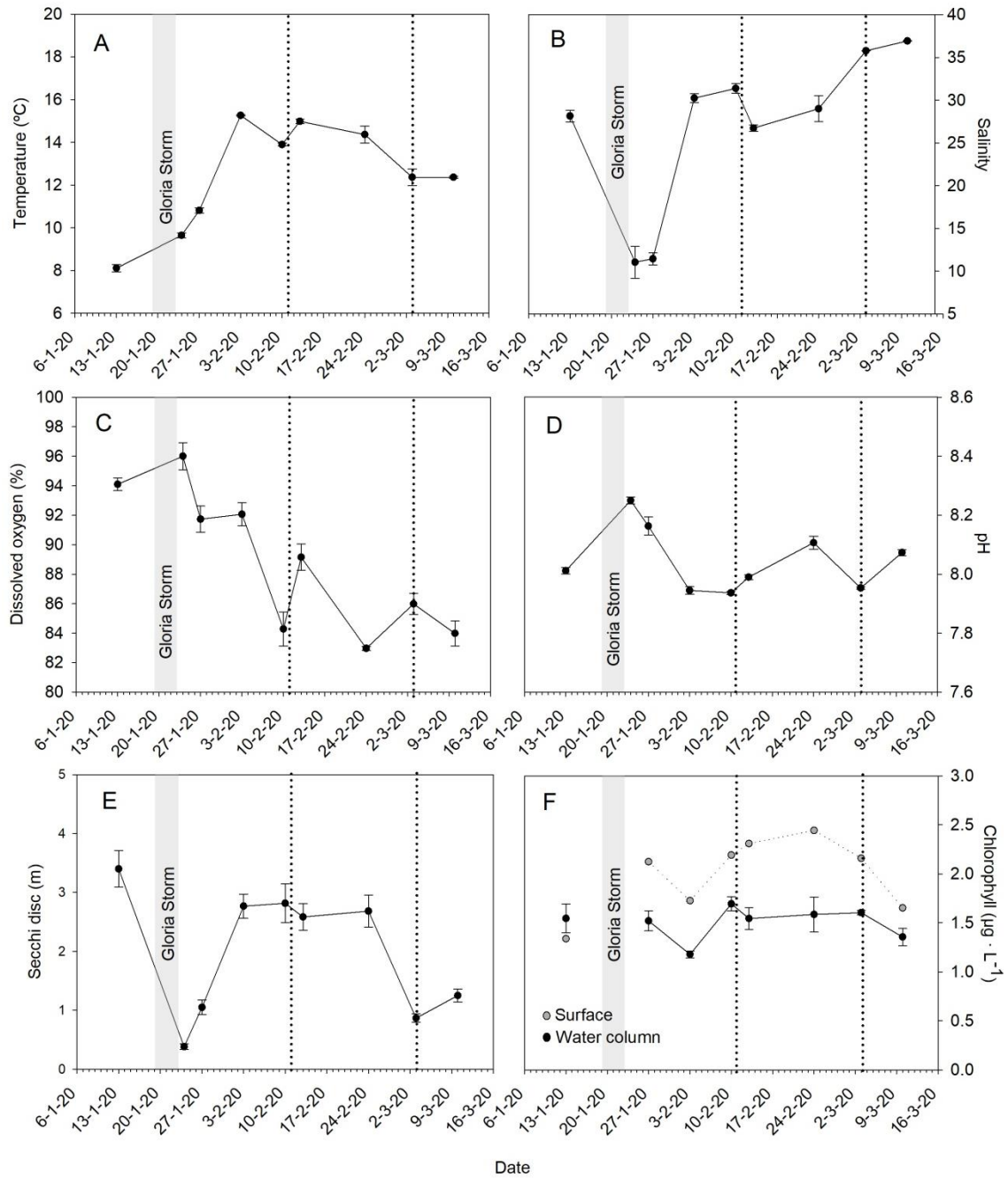




887

888 **Fig. 7**

889



890

891 **Fig. 8**

892 **Table 1.** Mortality patterns in Alfacs Bay. A) One-way RM-ANOVA for monthly cumulative  
 893 mortality of pen shells during the study period (January 2018 to March 2020) showing  
 894 differences among sampling times (within subjects) and zones (among subjects). Since the  
 895 Sphericity assumption was not meet, the Greenhouse-Geisser correction was used. B) Two-  
 896 way RM-ANOVA testing for differences in the abundance of living and dead individuals of  
 897 *Pinna nobilis* (juvenile and adults) in the impacted area of the bay (Zone 1 area closer to the  
 898 mouth of the bay). D= Dead, A= Alive; Significant results are indicated in **bold**.  
 899

<b>Alfacs Bay</b>						
A) One-way-RM-ANOVA	Type III SS	df	MS	<i>F</i>	<i>p</i>	
Time (Ti)	11.19	1.20	9.31	164.03	<b>0.000</b>	
Ti x Z	13.38	2.40	5.57	98.07	<b>0.000</b>	
Error (Ti)	0.409	7.207	0.057			
Zone (Z)	37.74	2	18.87	68.26	<b>0.000</b>	
Error (Z)	1.65	6	0.276			
LSD (Ti)	J18-Jun18> Jul 18> Aug18-Jun19> Jul19> Aug19>Sep19-Mar20					
LSD (Z)	Z1> Z2> Z3					
B) 2-way RM-ANOVA	Type III SS	df	MS	<i>F</i>	<i>p</i>	
Time (Ti)	0.00	1	0.00	0.00	1.000	
Ti x A	0.00	1	0.00	0.00	1.000	
Ti x IC	9.80	1	9.80	50.28	<b>0.000</b>	
Ti x A x IC	9.80	1	9.80	50.28	<b>0.000</b>	
Error (Ti)	30.40	156	0.195			
Age (A)	7.81	1	7.812	1.43	0.233	
Ind. condition (IC)	221.11	1	221.11	40.53	<b>0.000</b>	
A x C	4.51	1	4.51	0.82	0.364	
Error	850.95	156	5.45			
LSD (IC)	D> A					

900

901

902

903 **Table 2.** Mortality patterns in Fangar Bay. A) RM-ANOVA for monthly cumulative mortality of  
 904 pen shells during the study period from January 2018 to March 2020 (within subjects' effects).  
 905 Since the Sphericity assumption was not meet, the Greenhouse-Geisser correction was used.  
 906 B) RM-MANOVA testing for differences in the abundance of individuals of different conditions  
 907 (recently dead and living juvenile and adults, and the presence of old shells) in the four zones  
 908 of Fangar Bay at two times after Storm Gloria. LA= Living Adults, RDA= Recently Dead Adults,  
 909 LY= Living Young specimens, RDY= Dead young specimens, OS= Old Shells. Statistically  
 910 significant results are indicated in **Bold**.

911

<b>Fangar Bay</b>							912
A) RM-ANOVA		Type III SS	df	MS	F	p	913
Time (Ti)		3.853	1.112	3.466	93.138	<b>0.007</b>	914
Error (Ti)		0.083	2.223	0.037			915
Error		1.883	2	0.941			916
LSD (Ti)		Feb 2020> All months					917
<hr/>							918
B) RM-MANOVA		Type III SS	df	Wilk's λ	F	p	
Time (Ti)			3	0.390	36.987	<b>0.000</b>	919
Ti x Z			8	0.191	18.728	<b>0.000</b>	920
Zone	LA	836.30	3	278.77	18.89	<b>0.000</b>	921
	RDA	3711.42	3	1237.14	15.01	<b>0.000</b>	922
	LY	5.69	3	1.89	53.86	<b>0.000</b>	923
	RDY	87.12	3	29.04	16.95	<b>0.000</b>	924
	OS	3500.88	3	1166.96	21.27	<b>0.000</b>	925
Error	LA	1079.13	73	14.78			926
	RDA	6015.55	73	82.40			927
	LY	2.57	73	0.03			928
	RDY	125.02	73	1.71			929
	OS	4005.00	73	54.86			930

926

927 **Table 3.** Two-way ANOVA (Alfacs) and one-way ANOVA (Fangar), testing for differences in the  
 928 physicochemical variables of the bays. A) Temperature (°C), b) salinity, c) dissolved oxygen (%),  
 929 d) pH. In SNK of Alfacs Bay, significant differences among study zones are indicated. For  
 930 significant temporal variability (SNK) see Fig. 5. Statistically significant results are indicated in  
 931 **Bold.**  
 932

ANOVA	Alfacs				Fangar				
a) Temp	df	MS	F	p	e) Temp	df	MS	F	p
Date= D	25	315.78	3454.0	<b>0.000</b>	Date= D	25	139.60	8181	<b>0.000</b>
Zone= Z	2	0.27	0.0	0.992	Error	52	0.02		
Z x D	51	0.91	9.9	<b>0.000</b>					
Error	162	0.09							
b) Salinity	df	MS	F	p	f) Salinity	df	MS	F	p
Date= D	25	15.6	495	<b>0.000</b>	Date= D	25	71.87	1547	<b>0.000</b>
Zone= Z	2	10.4	6	<b>0.004</b>	Error	52	0.05		
Z x D	51	0.7	21	<b>0.000</b>					
Error	162	0.1							
SNK (Z)	Z1> Z2= Z3								
c) DO	df	MS	F	p	g) DO	df	MS	F	p
Date= D	2	94	1.18	0.308	Date= D	25	118.4	72.9	<b>0.000</b>
Zone= Z	25	505.69	95.89	<b>0.000</b>	Error	52	1.6		
Z x D	51	102.42	19.42	<b>0.000</b>					
Error	162	5.27							
d) pH	df	MS	F	p	h) pH	df	MS	F	p
Date= D	25	0.452	55.43	<b>0.000</b>	Date= D	25	0.088	1.62	<b>0.021</b>
Zone= Z	2	0.06	0.9	0.406	Error	52	0.054		
Z x D	51	0.027	3.41	<b>0.000</b>					
Error	162	0.008							

957